Order Number 1350780

Preformulation studies of melanotan-II

Lan, En-Ling, M.S.

The University of Arizona, 1992

U·M·I
300 N. Zeeb Rd.
Ann Arbor, MI 48106

Preformulation Studies of Melanotan-II

by

En-Ling Lan

A Thesis Submitted to the Faculty of the

Department of Pharmaceutical Sciences

In Partial Fulfillment of the Requirements
For the Degree of

MASTER OF SCIENCE

In the Graduate College

THE UNIVERSITY OF ARIZONA

1 9 9 2

STATEMENT BY AUTHOR

This thesis has been submitted in partial fulfillment of requirements for an advanced degree at The University of Arizona and is deposited in the University Library to be made available to borrowers under rules of the library.

Brief quotations from this thesis are allowable without special permission, provided that accurate acknowledgement of source is made. Requests for permission for extended quotation from or reproduction of this manuscript in whole or in part may be granted by the head of the major department or the Dean of the Graduate College when in his or her judgment the proposed use of the material is in the interests of scholarship. In all other instances, however, permission must be obtained from the author.

SIGNED: En-Ling Lan

APPROVAL BY THESIS DIRECTOR

This thesis has been approved on the date shown below:

James Blanchard — Sept. 17/92

James Blanchard
Professor of
Pharmaceutical Sciences

Date

ACKNOWLEDGEMENTS

I would like to express my gratitude to Dr. James Blanchard for his help and guidance during this thesis research and compilation. My appreciation is also extended to Dr. Michael Mayersohn and Dr. Sherry Chow for their suggestions and serving in my committee. I am grateful to Sydney Ugwu for his helpful assistance during my experimental work and data analysis. Thanks are also due to my friends who helped me to go through the most difficult time.

I especially thank my parents, sisters, and brother, without whose love, encouragement and invaluable support this thesis would not have been possible.

Table of Contents

Table of Contents (Continued)

List of Figures

List of Tables

ABSTRACT

Melanotan-II (MT-II) is a cyclic heptapeptide analogue of α-MSH (α-melanocyte stimulating hormone) which tans the skin rapidly and is currently being evaluated for the prevention of sunlight-induced skin cancers. In these preformulation studies, the degradation of MT-II followed apparent first-order kinetics. The degradation rate increased as the temperature or phosphate buffer concentration were increased. The pH-rate profile of MT-II degradation showed that MT-II was most stable at approximately pH 5. The degradation of MT-II was not affected by ionic strength. The pK_{a1} and pK_{a2} were estimated to be 6.53 and 11.74, respectively. The partition coefficient was studied at various pH values. The Δ log PC at pH 7.35 was 1.05 which indicated that MT-II could pass the intestinal membrane relatively easily. The preformulation data presented here can be used to help develop an appropriate dosage form for MT-II.

CHAPTER I
REVIEW OF THE LITERATURE

Problems in Peptide/Protein Drug Delivery

Introduction

Peptides and proteins are molecules consisting of two or more amino acids which are covalently linked together by amide bonds. They are the most abundant components of biological cells. There is no distinct borderline between the two groups of materials; most people agree that proteins are large molecules that usually contain at least 50 residues (Banga and Chien, 1988; Bailey, 1990). Some investigators suggest that molecules built of 100 or more amino acid residues be regarded as proteins and those containing fewer residues as peptides (Bodanszky, 1988). The most important feature of proteins is that they possess well-defined three-dimensional structures. Peptides, on the other hand, are rather small molecules (usually containing less than 50 residues), which do not generally possess a well-defined three-dimensional structure (Bailey, 1990). Peptides can be further differentiated into two groups; the term "polypeptide" refers to peptide molecules that contain about eight or more amino acids, whereas an "oligopeptide" is a peptide molecule with a chain of fewer than eight amino acids (Chien, 1992). Peptides and proteins can perform many roles-- for example, transport mediators, enzymes, hormones, antibiotics, interferons, etc. As a result of advances in biochemistry and genetic engineering over the last decade, several peptides and proteins have been produced successfully through recombinant DNA technology and synthesis, and they have become a major class of therapeutic agents. Peptide and protein drugs have many advantages over conventional drugs: they possess potent pharmacological effects, therefore, lower doses are needed. In

addition, they are highly specific and "natural", and thus cause fewer side effects. Unfortunately, because of their susceptibility to degradation by the strongly acidic environment and the proteolytic enzymes in the gastrointestinal tract, the systemic bioavailability of most peptides and proteins following oral administration is extremely low (usually less than 2%). Furthermore, peptides and proteins are high-molecular-weight macromolecules which do not easily permeate the intestinal mucosa. Even after successful gastrointestinal absorption, they can be further eliminated by first-pass metabolism in the liver. To date, most peptides and proteins are administered only by injection several times per day. This therapeutic regimen is risky due to the possibility of infection and the need for proper injection technique and is best administered under close medical supervision, therefore, compliance is poor. Thus, the successful development of peptide/protein drug delivery systems remains a significant and important challenge to pharmaceutical scientists.

Architectural Structures

There are four types of architectural features in proteins: primary, secondary, tertiary, and quaternary structures (Figure 1). With peptides, the molecular structure usually has considerable freedom of movement, and tertiary structure is rarely observed.

The primary structure is the covalent backbone including amide bonds and α-carbons. In other words, the primary structure is the order (or sequence) of the amino acid residues. The bond between the carbon atom of the carbonyl group and amide nitrogen has partial double bond character because of resonance. This would stabilize the amide bond and make the carbonyl carbon and oxygen atoms, the amide nitrogen and hydrogen and the two adjacent α-carbon atoms lie in approximately the same plane (Bodanszky, 1988).

Figure 1.
The Architectural Structures of Peptides and Proteins

A

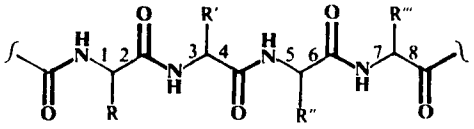

B

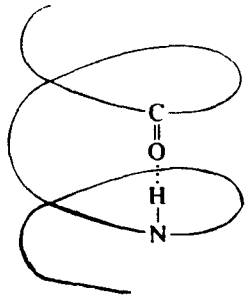

C

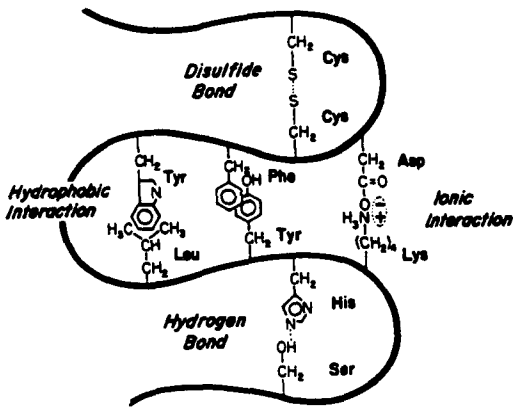

D

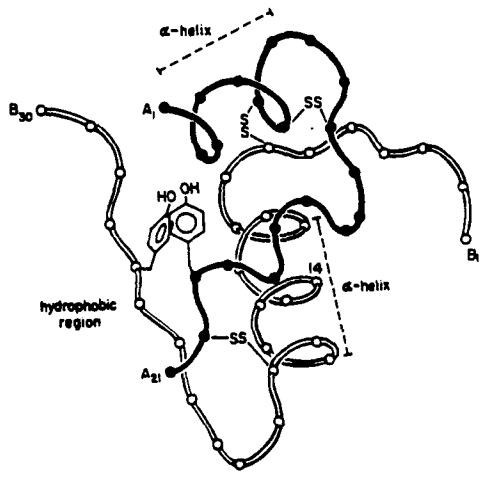

A: Primary Structure
B: Secondary Structure
C: Tertiary Structure
D: Quaternary Structure

The secondary structures refer to specific structural features within the molecule, which can be classified into three groups, i.e., α-helix, β-sheet, and reverse turns. The α-helix is a spiral structure stabilized by intramolecular hydrogen bonds between carbonyl oxygens and amide nitrogens which are four residues apart. The β-sheet is formed by two distinct stretches (two parts of the same chain) connected with each other through multiple hydrogen bonds. In reverse turns, a sharp change in the direction of the peptide backbone is stabilized by an intramolecular hydrogen bond between a carbonyl oxygen atom and a nearby amide nitrogen (Bodanszky, 1988).

The tertiary structure refers to a well-defined three-dimensional folding of the peptide chain. An important factor in folding is a non-polar interaction, often described as a hydrophobic bond. The functional groups on each of the amino acids and the sequence of the amino acids in the peptide chain determine the specific three dimensional folding of the protein molecule, which is referred to as the "conformation" of the protein. Hydrophobic residues, such as amino acids with aliphatic hydrocarbon groups (e.g., alanine and leucine) or with aromatic rings (e.g., phenylalanine and tryptophan), tend to inhabit the interior of the protein molecule. On the other hand, hydrophilic residues, such as amino acids with charged and/or polar groups (e.g., aspartic acid and lysine), tend to reside on the surface of the protein molecule and are in contact with the surrounding water. The hydrogen bonds and disulfide bonds can also contribute to tertiary structure (Bodanszky, 1988; Chien, 1992).

Quaternary structures occur in protein molecules having two or more polypeptide chains. The two or more "subunits" are linked through hydrogen bonds, polar or non-polar interactions to assemble into still larger structures. Not all proteins have quaternary

structures. This kind of aggregation seems to be related to a degree of conformational freedom (Bodanszky, 1988).

The delivery of peptides and proteins to the body is related to their architectural structures, not only because of their sizes and shapes, but also their hydrophilicity. The relatively high molecular weight and steric properties of polypeptides and proteins results in their poor penetration across biological membranes and pose unique basic formulation challenges. However, for an oligopeptide, the architectural structure is not so complicated, and the delivery problem is easier to solve.

Formulation Methods that Have Been Attempted

In recent years, controlled-release delivery systems and many nonparenteral routes such as the oral, nasal, pulmonary, ocular, buccal, sublingual, vaginal, rectal, and transdermal routes have been studied to minimize the health hazard of constant injection (Lee, 1991). Without coadministration of an absorption-promoting adjuvant, the nonparenteral routes are known to generally achieve a much lower bioavailability than parenteral administration for most peptides and proteins. However, by adding absorption enhancers and modifying the dosage form, the absorption may be increased to a satisfactory level.

Coadministration with absorption enhancers including protease inhibitors and permeability promoters is the most common method to improve the absorption of peptides and proteins. Many compounds have been reported as permeability promoters for insulin and other proteins, including surface-active agents, bile acids, saponin, phospholipids, organic alcohols, fatty acids, salts, amines, and fats (Rytting, 1989). Examples of protease

inhibitors include: α-aminoboronic acid derivatives which are used as potent reversible inhibitors of aminopeptidases in the nasal cavity (Hussain et al., 1989).

Controlled-release delivery systems for peptide and protein drugs may offer another approach to improve the bioavailability and prolong the duration of response. Liposomes and biodegradable polymers are often used as controlled-release vehicles. They have been studied for use via parenteral, as well as nonparenteral routes, to modulate the extremely short-acting biological functions. Implantable inserts are also regarded as a controlled-release delivery system (Banga and Chien, 1988).

The prodrug approach is another method which has been evaluated for improving the systemic delivery of peptides and proteins. The prodrug concept involves the chemical modification of the pharmacologically active compound into a bioreversible form with the aim of changing its pharmaceutical and/or pharmacokinetic character and thereby enhancing its delivery, efficacy and therapeutic value. Regeneration of the active drug occurs in vivo by either enzymatic hydrolysis or simply by chemical processes (Chan and Po, 1989). For example, N-acylation of the imidazole group of the histidine residue can improve the lipophilicity of thyrotropin-releasing hormone (TRH), and can also increase the resistance to cleavage by the TRH-specific pyroglutamyl aminopeptidase serum enzyme (Bundgaard and Møss, 1990). Saffran et al. (1986) developed an interesting approach to oral delivery. They coated drug particles with polymer crosslinked with an azoaromatic group that formed an impermeable film and afforded protection to acidic and enzymatic degradation in the intestinal lumen. The polymer is degraded by microflora present in the large intestine, releasing the compound for absorption. This approach was successfully demonstrated for vasopressin and insulin (Saffran et al., 1986).

Bioadhesive polymers/copolymers have been used as platforms for peptides and proteins in nonparenteral routes of administration. They can be localized in specified regions and may also prolong the residence time, and ensure an optimal contact with the absorbing surface, thereby enhancing the bioavailability of peptides and proteins (Junginger, 1990). Nanocapsules and nanoparticles have been considered a tool for oral absorption of peptides. They were demonstrated to be able to pass from the intestinal lumen to the blood compartment by means of a paracellular pathway (Damge et al., 1988). The technique of iontophoresis was reported in transdermal delivery. This method delivers ions and charged molecules into the body by the use of electric current (Chien et al., 1989).

In addition to the previous approaches, there are too many other trials to describe each in detail. Above all, the ultimate challenge in peptide and protein delivery is to understand the requirements to be met in order to successfully deliver peptides and proteins in effective and convenient delivery systems, especially for the oral route, which is expected to be more readily accepted by patients than any of the alternative routes under investigation.

Melanotan-II

History

The α-melanocyte-stimulating hormone (α-MSH or α-melanotropin) is a tridecapeptide (Ac-Ser-Tyr-Ser-Met-Glu-His-Phe-Arg-Trp-Gly-Lys-Pro-Val-NH_2) that is synthesized and secreted by the pituitary gland of vertebrates. It stimulates pigment-

producing cells (melanophores or melanocytes) to synthesize melanin (Hadley et al., 1989). Melanotan-II (Ac-[Nle^4,$\overline{Asp^5,D\text{-}Phe^7,Lys^{10}}$] α-$MSH_{4\text{-}10}$-$NH_2$) is an analogue of α-MSH.

After the isolation and primary structure determination of α-MSH in the 1950s, many investigators initiated studies of the synthesis of this peptide. These syntheses then led to the initiation of structure-activity studies in several laboratories. In 1980, Sawyer, Hruby and co-workers first synthesized a more potent form of melanocyte stimulating hormone. They found that with a substitution of Met for Nle in position 4 and using the D form of Phe in position 7, a more potent analogue of α-MSH could be sythesized (Sawyer et. al.,1980). This potent analogue, Ac-[Nle^4, D-Phe^7] α-MSH, which can tan the skin without sunlight exposure, was named "melano-tan"(melanotan-I). It was determined to be more potent than native α-MSH in the in vitro frog and lizard skin bioassays and had very prolonged biological activities in vitro and in vivo (Sawyer et. al.,1980; Hadley et. al.,1981). The fragment analogue, Ac-[Nle^4, D-Phe^7] α-$MSH_{4\text{-}10}$-NH_2, also proved to be particularly potent in most bioassays (Marwan et al., 1985). Hruby and co-workers noted that replacement of Gly^{10} and Met^4 with cysteines, followed by oxidation to the disulphide, would lead to a pseudoisosteric substitution, and synthesized [$\overline{Cys^4,Cys^{10}}$] α-MSH. This peptide was found to be more than tenfold more potent than α-MSH in the in vitro frog skin bioassay and at least twofold more potent in the in vitro lizard skin bioassay (Chauen et al., 1987). Since [Nle^4, D-Phe^7] α-MSH and a cyclic analogue [$\overline{Cys^4, Cys^{10}}$] α-MSH provided higher potency, they were used as lead compounds. Later, Al-Obeidi and co-workers (1989) also observed that a modification of Glycine in position 10 for lysine would permit the formation of a salt bridge with the Glu (or Asp) in position 5. The connection of residue 5 and residue 10 caused a reverse turn in the His-Phe-Arg-Trp part of the molecule, as well as a segregation of lipophilic and hydrophilic side-chains to opposite

faces of the molecule relative to the ring. Utilizing this information and previous results, Hruby and Al-Obeidi completed the design and synthesis of a new, smaller peptide, Ac-[Nle^4,Asp^5,D-Phe^7,Lys^{10}] α-MSH$_{4-10}$-NH$_2$, which was found to be superpotent in both the lizard skin (90-fold more potent) and melanoma tyrosinase (100-fold more potent) assays relative to α-MSH and which also exhibited prolonged biological activity. The new cyclic lactam bridged analogue was named "melanotan-II" (Al-Obeidi et al., 1989; Hruby et al., 1991).

In addition to the superpotent and prolonged-acting characteristics, MT-II is less charged compared to the linear homologue and other related α-MSH analogues due to the lactam bridge between positions 5 and 10 which replaces two charged groups. The molecule may therefore be more lipophilic and may possibly be absorbed by nonparenteral routes better than other more highly charged melanotropins.

Physicochemical Properties

Figure 2 shows the structure of MT-II, which has a formula of $C_{49}H_{71}N_{15}O_9$ and a molecular weight 1025.0 (Al-Obeidi et al., 1989). It is synthesized as a diacetate salt form. It is a white amorphous powder which is quite soluble in water. This heptapeptide has two basic amino acids, histidine and arginine, which are positively charged at acidic pH. Those are the sites where the acetate salt is formed. Therefore, we can predict the approximate pKa values for MT-II from the pKa of histidine which is around 6 and the pKa of arginine, which is around 12. Because it is a new compound and still in the experimental stage, no previous data about its physicochemical properties are available.

Figure 2.

Chemical Structure of Melanotan-II

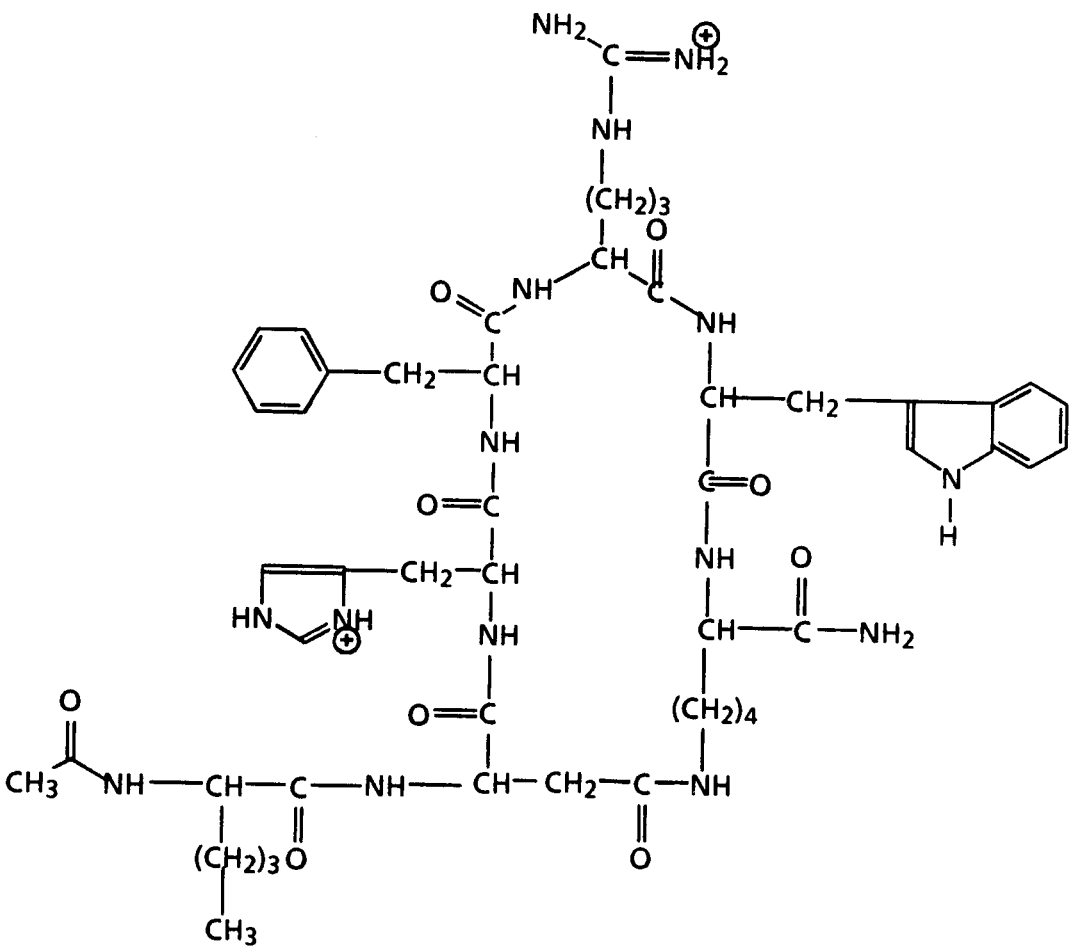

Ac-[Nle^4,Asp^5,D-Phe^7,Lys^{10}] α-MSH$_{4\text{-}10}$-NH$_2$

Clinical Application of Melanotan-II

A novel tanning technique may be of interest for its cosmetic effect, but besides its cosmetic potential, MT-II is a potentially more important agent for its therapeutic uses. Melanotan-II is currently being studied primarily as a skin cancer prevention agent.

It has been estimated for 1991 that over 600,000 new cases of skin cancer occurred in the United States. Skin cancers are more common among individuals with lightly pigmented skin who live at latitudes near the equator. As the ozone layer becomes more and more depleted, the incidence of skin cancer is increasing. However, the incidence in blacks is low and shows no such increase. This phenomenon is ascribed to the higher amount of melanin within the epidermis in blacks. α-MSH acts on pigment-producing cells which synthesize melanin within the epidermis. The colored polymer, melanin, can absorb a wide range of ultraviolet (UV) and visible light and hence protect the skin from UV radiation injury. Therefore, increasing melanin levels in the skin might afford protection against the harmful effects of ultraviolet light (Nacht,1991; Levine et al., 1991; American Cancer Society, 1991).

As described previously, melanotan I and II can induce melanin production, and have been shown to possess much higher potency than α-MSH. These two compounds have been approved by the FDA (Food and Drug Administration) for studies in humans. Melanotan studies are now at the phase-1 stage; those studies are directed toward determining whether the product is effective and safe to use. The toxicity of MT-I has been studied in several rodent species. Mice were administered up to 2 mg/kg of MT-I daily and weekly over 4 or 12 weeks by both topical application (in 90% DMSO) or by intraperitoneal injections (in physiologic saline). At the end of this period, no toxic effects

were observed in various organs, on hematologic indices, or on weight gain (Dorr et al.,1988).

Levine et al.(1991) studied the induction of skin tanning of melanotan-I in humans. Each male subject received 10 subcutaneous injections of either a purified melanotan-I preparation (0.08 mg/kg of the body weight per injection) or saline over 12 days. The double-blind test showed that human skin darkened in response to melanotan given by subcutaneous injection. In this study, skin tanning was shown to be possible without the potentially harmful exposure to ultraviolet radiation. MT-I did not show any toxic effects in human volunteers at the experimental doses (Levine et al.,1991).

MT-I has also been studied using transdermal delivery. In vitro studies have demonstrated the delivery of this peptide across mouse and human skin (Hadley et al., 1987; Dawson et al., 1990). However, it was reported that MT-I can not cross rat skin in an in vitro model system (Dawson et al., 1988).

MT-II has been reported to show greater potency, prolonged activity, and stability against enzyme inactivation than MT-I (Hadley et al., 1989). Its toxicity was studied in adult rats by administering 0.5 mg/kg/day of MT-II by either the oral or subcutaneous route for 30 days. No evidence of toxicity was found. From the results of the relative non-toxicity to rats, a daily dose of approximately 0.4 mg/kg/day was used for initial clinical trials in humans (Dorr and Dawson, 1989). The double-blind, phase 1 study to determine the safety and efficacy of subcutaneous MT-II in human is currently being investigated. A recent study (Griego and Levine, 1992) demonstrated the ability of MT-II to induce skin tanning in humans without sun exposure.

Assays for Melanotan-II

To date, very few assays have been reported for melanotan-II. The presence of this peptide in biological fluids was mainly monitored using frog skin and lizard skin bioassays. The changes of skin darkness were monitored by a photovolt reflectometer and recorded as differences from the intial base line value (Hadley, 1989). However, these bioassays are only semi-quantitative, nonspecific, variable and expensive. HPLC procedures have been reported by Cody et al. (1984) and Lebl et al. (1984) for the separation of mixtures of other cyclic α-melanotropic peptides. These procedures were primarily developed for preparative purification and were aimed at examining the chromatographic behavior and mechanism of separation of mixtures of these analogues (Cody et al., 1984; Lebl et al., 1984).

Recently, one quantitative assay for measuring melanotan-II in biological fluids was developed by Ugwu and Blanchard (1992). They reported a senstive, specific, reproducible, and stability-indicating HPLC assay for MT-II in plasma using a reversed-phase column at 35 °C and phosphate buffer/ acetonitrile as mobile phase. The same HPLC conditions are expected to give good results for measuring MT-II in aqueous solution since the composition of aqueous solutions is simpler than biological fluids.

Preformulation

Definition

Preformulation testing is the first step in the rational development of dosage forms of a drug substance. It can be defined as an investigation of the physical and chemical properties of a drug substance alone and when combined with excipients. The overall

object of preformulation testing is to generate information useful to the formulator in developing stable and bioavailable dosage forms that can be mass produced (Wadke et al., 1989). It may be also described as a stage of development during which the pharmacist characterizes the physical-chemical properties of the drug substance in question which are considered important in the formulation of a stable, effective and safe dosage form (Ravin and Radebaugh, 1990). Since preformulation studies enabled one to make critical decisions as to which form of the active compound should be recommended for the formulation design and to optimize the performance of drug products, it eventually became part of official requirements for Investigational New Drug Applications (INDs) by the Food and Drug Administration (FDA).

In the preformulation stage, such parameters as stability, aqueous solubility, pKa, partition coefficient, drug permeability, dissolution behavior, and standardization of the physical properties are evaluated. Unlike usual physicochemical studies, an abundance of material is not usually available at this stage. Therefore the investigator must settle for good estimates. The type of information needed will depend on the dosage form to be developed. Not all the preformulation parameters are determined for every new compound. For example, a detailed investigation of dissolution is not warranted for a very soluble compound (Wadke et al., 1989). Review of the physical-chemical properties of the test compounds and related compounds would help to determine the most appropriate preformulation program.

Stability

A successful product must survive processing and storage over the claimed shelf life without excessive loss of potency or excessive increase in the level of decomposition

products. In the preformulation stage, the physicochemical stability of the compound may be considered the primary biopharmaceutical item and must be evaluated to assure its quality and safety. It may be influenced by a wide range of environmental factors such as: temperature, pH, buffer concentration and ionic strength.

The degradation of a chemical compound, such as aspirin, may be readily detected by using HPLC or other stability-indicating assays. The degradation or denaturation of a protein is much more complicated because the stability of peptides and proteins is directly related to their architectural structures, and the denatured products are not readily detectable. The degradation of proteins and peptides can be divided into two main categories, one involves breaking a covalent bond and the other does not. The latter process is often referred to as denaturation. Six major reactions, which involve breaking covalent bonds, can participate in protein degradation: hydrolysis, imide formation, deamidation, oxidation, disulfide exchange, and photodecomposition. Denaturation is the disruption of protein conformation, which may cause partial or complete loss of biological activity. Peptides have no tertiary structure and are therefore not susceptible to denaturation by any means (Wang and Hanson, 1988).

Fortunately, Melanotan-II is a relatively simple peptide which contains seven amino acids and is therefore not likely to exhibit a complicated degradation pattern. Therefore, one can reasonably expect the stability behavior of MT-II to be similar to that of a normal chemical compound.

Effect of Temperature on Stability

Actual elapsed time (i.e., real time) stability studies are the most reliable demonstration of the shelf life of a new compound, but they are time-consuming. In preformulation, the length of time required for stability studies often renders them impractical. Therefore, a reliable alternative to real time stability testing is to use accelerated degradation. The most common acceleration method is to elevate the temperature, and to predict rates of degradation based on the Arrhenius equation because the degradation rate usually increases as the temperature is raised.

The rate constant of many chemical reactions can be empirically related to the absolute temperature by the Arrhenius equation:

$$K = A\, e^{-Ea/RT} \qquad \text{Eq.(1)}$$

where K is the rate constant, A is the preexponetial constant, Ea is the experimental activation energy, R is the gas constant, and T is absolute temperature. Equation 1 can be written as :

$$\log K = \log A - (Ea/2.303\, RT) \qquad \text{Eq.(2)}$$

Equation 2 will yield a linear plot of log K versus 1/T which is called an Arrhenius plot. From the slope of an Arrhenius plot the activation energy is calculated. The preexponetial constant A can then be calculated from the intercept. The data obtained at elevated temperatures may be extrapolated using the Arrhenius plot to determine the degradation rate at a lower temperature (Connors, 1981). This extrapolation method of course assumes that the degradation mechanism does not change over the temperature range extrapolated (Pearlman and Nguyen, 1992). Although it has been reported that peptide and protein

drugs are usually considered not to follow the Arrhenius equation, some simple peptides have been shown to give a linear Arrhenius plot. For example, for gonadorelin and triptorelin, which are both decapeptides, the Arrhenius plots have been reported to be reasonably linear between 30 and 80°C (Helm and Müller, 1990).

Effect of pH on Stability

The degradation rates in aqueous solution are often markedly dependent on the solution pH. When examining the degradation rates at different solution pH values, the data can be presented as plots of K against pH or log K against pH; both forms of data display are called pH-rate profiles. The primary goal of the pH-rate profile is to elucidate the optimal pH range for stability. The manner of the analysis is to locate characteristic features of the pH-rate curve (linear segments, maxima, minima, and inflection points), and to relate the value of pH at which they occur to the parameters of the equation (Connors, 1981). A general hypothetical rate equation can be written as Eq. (3):

$$K_{obs} = K_{H^+}[H^+]^n + K_0 + K_{OH^-}[OH^-]^m \qquad \text{Eq.(3)}$$

where $[OH^-] = K_W/[H^+]$; K_W is the ion product of water, equal to 1.00×10^{-14} at 25°C. Consider the very low pH region, where $[H^+]$ is large. Equation 2 can be written as

$$K_{obs} = K_{H^+}[H^+]^n \qquad \text{Eq.(4)}$$

since the term representing acid-catalysis will be much larger than the other terms at low pH. When the data are plotted as log K versus pH (at low pH), a slope of $-n$ should be found. In this way the order with respect to hydrogen ion can be determined. Once n has been determined, K_{H^+} can be found from the data at low pH by applying Eq. (4). By a

similar development, the order with respect to hydroxyl ion *m* and K_{OH^-} at high pH can also be determined. Finally, K_0 can be found from data in the intermediate pH range by using Eq. (3) and the known values of *m*, *n*, K_{H^+}, and K_{OH^-}. With the estimated parameters *m*, *n*, K_{H^+}, K_0, and K_{OH^-}, Eq. (3) can be then used to calculate K_{obs} as a function of pH. If the slopes of the straight line segments at low and high pH are -1 and +1, respectively, this indicates that the rate equation contains terms first order in $[H^+]$ and in $[OH^-]$. In other words, it is specific acid catalysis by hydrogen ion and specific base catalysis by hydroxyl ion. If the slope is not -1 or +1, it indicates that the compound degrades by several different pathways, each with its own pH dependence and true catalytic coefficient. The parameters can also be determined by a nonlinear least-squares computer program(Carstensen,1990). There is no certain shape for log K-pH profile or K-pH profile. It can be a parabolic plot as seen with luteinizing hormone releasing hormone (LHRH) (Powell et al., 1991), or it can be a sigmoidal plot as with levothyroxine (Won, 1992).

Effect of Buffer Concentration on Stability

Buffer salts are commonly used in the formulation of pharmaceutical solutions to resist change in the effective acidity or alkalinity of a medium upon the addition of increments of acid or base. Although these salts tend to maintain the pH of the solution at a constant level, they can also catalyze the degradation of the active ingredient. Therefore, it is necessary to evaluate the effect of buffer concentration on the stability of the preparation in addition to the effect of hydrogen and hydroxyl ion concentrations. Common buffer salts such as acetate, phosphate, citrate, and borate have been found to have catalytic effects on the degradation rate of drugs in solution.

To determine whether a particular formulation is catalyzed by the buffer system employed, the ionic strength is kept constant, and the concentration of buffer is altered, while the ratio of the buffer salts is kept constant to maintain the pH. If the degradation reaction is found to be influenced by the different concentrations of the buffer, then the reaction is considered to be general acid and base catalyzed. In such a case, the concentration of the buffer should be kept as low as possible to diminish this catalytic effect (Lachman et al., 1986).

Effect of Ionic Strength on Stability

The Debye-Hückel equation is used to describe the relationship between the rate constant and the ionic strength (μ). It is often obeyed in solutions with μ values up to 0.01. Because most pharmaceutical investigations are conducted at ranges of $\mu>0.01$, the Debye-Hückel equation is modified to the following equation:

$$\log Kobs = \log K_0 + 2Q \cdot Z_A Z_B [\sqrt{\mu}/(1+\sqrt{\mu})] \qquad \text{Eq.(5)}$$

where Kobs is the observed rate constant, K_0 is the rate constant at $\mu=0$, Q is a constant for a given solvent and temperature, Z_A and Z_B are the charges on species A and B, respectively, and μ is the ionic strength. When log Kobs is plotted versus $\sqrt{\mu}/(1+\sqrt{\mu})$, the slope shows the effect of ionic strength (salt effect) on degradation. (Freeke Hamelijnck et al., 1992)

The ionic strength can also be interpreted with respect to polarity. The polarity of a solvent is related to its ability to solvate charged species. An increase in ionic strength (by

increasing the salt concentration) corresponds to an increase in solvent polarity. In the transition-state theory, we assume an equilibrium between the initial and transition states:

$$A + B \leftrightarrow M^{\ddagger} \rightarrow \text{Products} \qquad \text{Eq.(6)}$$

If the transition state is more polar than the initial state, then an increase in solvent polarity will increase the rate. If, on the other hand, the transition state is less polar than the initial state, an increase in solvent polarity will decrease the rate. This can be applied to four types of bimolecular reactions.

(a) Neutral nonpolar reactants giving neutral nonpolar products: A change in solvent polarity will have little effect on the rate since the transiton state is presumably nonpolar.

(b) Neutral reactants giving charged products: An increase in solvent polarity should result in an increase in rate, because the transition state will be more polar than the initial state.

(c) Neutral molecule-ion reactions: The transition state will be less polar than the initial state. Thus an increase in solvent polarity will decrease the rate.

(d) Ion-ion reactions: If the reactants are two ions of opposite charge, then the transition state will be less polar than the initial state. An increase in solvent polarity will decrease the rate. If the two ionic reactants have the same charge, the opposite conclusion is reached (Connors, 1981).

pKa Values

Most drugs used today are rather complicated organic molecules, a majority of which can undergo ionization under physiological pH conditions. The degree of ionization of a drug in the body is of prime interest to the pharmacist because it may be intimately related to a number of important properties, such as its absorption rate through a biological membrane, its rate of degradation, the overall pharmacological activity of the drug, etc.. The degree of ionization of a drug is primarily controlled by two parameters, i.e., the pH of the solution into which the drug is placed, and the pKa of the drug. Thus, pKa determination becomes an important part of preformulation.

By far the most convenient method for the determination of pKa is potentiometric titration using a glass electrode. Using a microburet, the titrant is added in equal portions to the sample solution. After each addition, the pH is determined precisely. The pKa can be determined from the inflection points of the plot of pH versus titrant volume. However, using the potentiometric titration method it is difficult to determine the pKa of very weak acids or very strong bases, particularly substances with a pKa of 11 or more because CO_2 becomes an interfering substance at high pH values. In addition, in the pH range 12-14 all types of glass electrode are inaccurate. (Albert and Serjeant, 1971)

Another widely used method to determine ionization constants is by ultraviolet or visible spectrophotometry. It is an ideal method when a substance is too insoluble for potentiometry, or when its pKa value is particularly low or high. Using the spectrophotometric method, the ratio [ionized form]/[nonionized form] can be determined in a series of buffers of different pH values. The pKa can then be found using the Henderson-Hasselbalch equation:

$$pH = pKa + \log [\text{ionized form}]/[\text{nonionized form}] \text{.....for acids} \quad \text{Eq.(7)}$$

$$pH = pKa + \log [\text{nonionized form}]/[\text{ionized form}] \text{.....for bases} \quad \text{Eq.(8)}$$

When expressed in terms of absorbance, Eq.(7) and Eq.(8) can be written as follows:

$$A_T = [Au + Ai \cdot 10^{(pH-pKa)}]/[1 + 10^{(pH-pKa)}] \text{.....for acids} \quad \text{Eq.(9)}$$

$$A_T = [Au + Ai \cdot 10^{(pKa-pH)}]/[1 + 10^{(pKa-pH)}] \text{.....for bases} \quad \text{Eq.(10)}$$

where A_T, Au, and Ai represent the total absorbance of the solution, the absorbance of its unionized form, and the absorbance of its ionized form, respectively.

Partition Coefficient

When a solute is added to two immisicible liquids that are in contact with each other, it will distribute itself between the two phases in a fixed ratio. This ratio is known as the partition coefficient (Wadke et al.,1989). The partition coefficient is used in the pharmaceutical sciences to correlate and predict the biological activity of a compound. Many studies have shown that the ability of the solute to partition into the cell membrane can be related to its partition coefficient in an organic solvent. It has been demonstrated that the partitioning behavior of a solute between n-octanol and water is a good predictor of its permeability across a variety of cell membranes and thus octanol serves as a good reference solvent (Hansch and Dunn, 1972).

However, good correlations between permeability and octanol-water partition coefficients can only be found for non-peptidic solutes, which are more lipophilic, since for these molecules the principal route for absorption is passive diffusion across the cell

membranes, and the principal driving force for transfer from water to the membrane will be the well known hydrophobic effect. Other factors which are important for passive transcellular flux include surface area, specific interactions and blood flow (Burton, et al., 1991).

For peptide or protein drugs, which contain many polar functionalities, there is no obvious relationship between permeability and the partition coefficient. For a polar peptide to cross the epithelium, there are two distinctly different pathways possible; the transcellular or the paracellular route. The absorption of peptides is therefore not simply related to their lipophilicity. In one study, it was reported that the hexapeptide analog renin inhibitor, SQ 71038, gave very low blood levels in the rat after oral administration even though the log PC was quite high (Ruwart et al., 1989). Conradi and co-workers (1991) studied the influence of peptide structure on transport across Caco-2 cells and found no significant relationship between permeability and the octanol/water partition coefficient. Their results suggested that either the increased size of the molecule, or the anticipated increase in energy required to desolvate the peptide in order for it to enter into the membrane with increasing amino acid number, could be more important than octanol solubility in determining the permeability of peptides (Conradi, et al., 1991). In the study by Burton and co-workers (1991), the permeability of peptides through Caco-2 cell monolayers was investigated Their results suggested that the number of polar groups on the molecules, which presumably require desolvation before transfer of the peptide into the cell membrane, was a principal determinant of transport. Therefore, the absorption of peptide drugs cannot be predicted solely by the partitioning behavior of a peptide between n-octanol and water (Burton et al., 1991). The authors suggested that by considering the hydrogen bonding effect, the observed partition coefficient would be more predictive. The principal solute-water forces which make the solute stay in water are hydrogen bonding of

water with the polar functionalities in the solute. The entropic component against hydrogen bonding is commonly known as the hydrophobic effect which arises from the dissolution of non-polar solutes in water. Therefore, the hydrophobic effect favors the transfer of solute out of water and into the membrane, while opposing this is the unfavorable desolvation energy required to break hydrogen bonds between water and peptide in order for the solute to enter the presumably non-hydrogen bonding interior of the membrane. Thus the membrane partition and permeation will be a balance of these two opposing tendencies. Since octanol is a hydrogen bonding solvent, the desolvation energy associated with breaking the amide-water bonds can be partially offset by the formation of amide-octanol bonds, thus the overall energy required for the desolvation step in the transfer process will be smaller than in the real situation in the intestine.

One simple experimental technique for measuring the partition coefficient of the peptides was described (Burton et al., 1991). This method assumes that the hydrophobic effect will be similar in two solvent types, one which can form hydrogen bonds with the peptide (e.g., octanol), and one which cannot (e.g., isooctane). Therefore the difference in partitioning will represent the ability of the organic solvent to accommodate the hydrogen bonding requirement of the solute and be a direct measure of the desolvation energy:

$$\Delta \log PC = \log PC_{\text{hydrogen bonding solvent}} - \log PC_{\text{non-hydrogen bonding solvent}} \qquad \text{Eq.(11)}$$

Using octanol as the hydrogen bonding solvent and isooctane as the non-hydrogen bonding solvent, a good correlation was found between Δ log PC and permeability for several peptides. This technique may therefore be useful for assessing the absorption potential of new peptide entities. (Burton et al., 1991, Burton et al., 1992)

Binding Problems of Peptides/Proteins with Glassware

The adsorption of proteins and peptides onto glass surfaces has been reported. If neglected, it can cause a large experimental error. This phenomenon is particularly significant at low concentrations of peptides/proteins in aqueous solution. The adsorption of peptides/proteins to glass has been ascribed to ionic amine-silanol bonding (Mizutani and Mizutani, 1978). Siliconization (silanization) of glassware is a recommended procedure for minimizing adsorption. The silicone coating on the glass surface provides a "hydrophobic type" barrier and hence eliminates the silanol-amine interactions which are considered to be the driving force in adsorption of amines and proteins onto glass. In a study by Anik and Hwang (1983), a decapeptide derivative of the luteinizing hormone releasing hormone (LHRH), showed no loss from solutions in contact with a silanized glass surface (Anik and Hwang, 1983). However, silicone-coated glass has been reported to adsorb the hormone secretin (Mizutani, 1981). On coated glass, proteins are adsorbed mainly by hydrophobic bonding between the aliphatic residues on proteins and silicone residues on coated glass (Mizutani,1981).

There is no totally satisactory method to prevent peptide/protein adsorption, nor a standard for silicone coating. Substituting plastic material which has a lower adsorption potential than glass is a good way to avoid the adsorption problem. In addition, a control experiment to correct the error caused by adsorption is recommended.

CHAPTER II

STATEMENT OF THE PROBLEM

In recent years, many bioactive peptides and proteins have been evaluated for use in therapy of a variety of diseases. The ultimate clinical utility of these peptide and protein drugs will depend on the development of suitable drug-delivery systems. Before the design of such formulations, the physicochemical properties of the drug should be determined. Melanotan-II (MT-II) has been evaluated for use in therapy of skin cancer. Its potential therapeutic importance prompted us to undertake a study of the chemical stability and degradation kinetics of this peptide in aqueous solution, as no previous data were available. The purpose of this study is to investigate the effect of temperature, pH, buffer concentration, and ionic strength on the stability of MT-II. The pKa values and partition coefficients of MT-II were also determined. Data obtained in this study will be used to develop a stable oral dosage form of MT-II for animal and clinical studies. Since the quantity of Melanotan-II available is small and because the Melanotan is made as an amorphous diacetate salt form, which is highly water-soluble, the solubility will not be determined in this study.

CHAPTER III

Experimental Materials and Methods

Reagents

Buffer solutions were prepared using potassium phosphate monobasic (analytical grade, J.T. Baker Chemical Company, Phillipsburg, NJ) and potassium phosphate dibasic (analytical grade, J.T. Baker Chemical Company, Phillipsburg, NJ). Purified Melanotan-II (99% pure) was obtained from Dr. Victor Hruby of the Department of Chemistry, The University of Arizona. Octanol was analytical grade and was purchased from Aldrich Chemical Company (Milwaukee, WI). Isooctane was analytical grade and was purchased from J.T.Baker Chemical Company (Phillipsburg, NJ). The water was obtained from a millipore filter system (Millipore Corp., Bedford, MA).

HPLC Conditions

The HPLC system consisted of a solvent delivery pump (IsoChrom, Spectra-Physics), an injection valve (Altex Model 210) fitted with a 50-µl loop, a Zorbax C8 column (10 um, 4.6 mm x 25 cm, DuPont Instruments, Wilmington, DE), a Co-Pell ODS precolumn (Whatman, Clifton, NJ), a variable-wavelength detector (Model 100-30, Hitachi/Spectra-Physics, Fremont, CA). Each injection was made with a 100-µl syringe (Model 702-SNR, Hamilton, Reno, NV) into the injection valve. The flow rate was 1.0 ml/min, the chart speed was 0.5 cm/min, and the sensitivity was set at 0.02 AUFS.

Equipment

Polypropylene tubes (12x75 mm, Falcon, Oxnard, CA) were used for sample preparation instead of glass tubes to avoid binding problems since peptides are known to bind avidly to glassware. The oven used to maintain temperature was a Model 1540 from VWR Scientific Inc. (Philadelphia, PA) The pH values of all solutions were measured on a digital pH meter (Model 130, Corning Glass Works, Medfield, MA).

The apparatus for partition coefficient measurements was a Mixxor separatory cylinder (Lidex Technologies Inc., Bedford, MA). It is an unique apparatus. The Mixxor (Figure 3) consists of a graduated glass mixing chamber into which fits a glass piston containing an axial channel. The axial channel leads to an upper reservoir, capped by a screw cap, and surrounded by a plastic retaining ring. There are four steps to using this apparatus. The two phases are poured into the upper reservoir (Step 1), the piston is then moved slowly up and down for an appropriate number of times (Step 2), the piston is then completely depressed into the mixing chamber, the screw cap is loosened, and the liquid is allowed to separate (Step 3), The retaining ring is then held to the top of the mixing chamber, the piston is positioned so that only the upper phase is contained in the reservior, and the upper phase is poured off (Step 4).

Methods

Preparation of Buffer Solution

0.1 M phosphate buffer was prepared by adding 17.42 g of dibasic potassium phosphate to 1 L of purified, deionized water and the pH value was adjusted to pH 2.2 with phosphoric acid.

Figure 3.

Schematic Diagram of Mixxor Separatory Cylinder

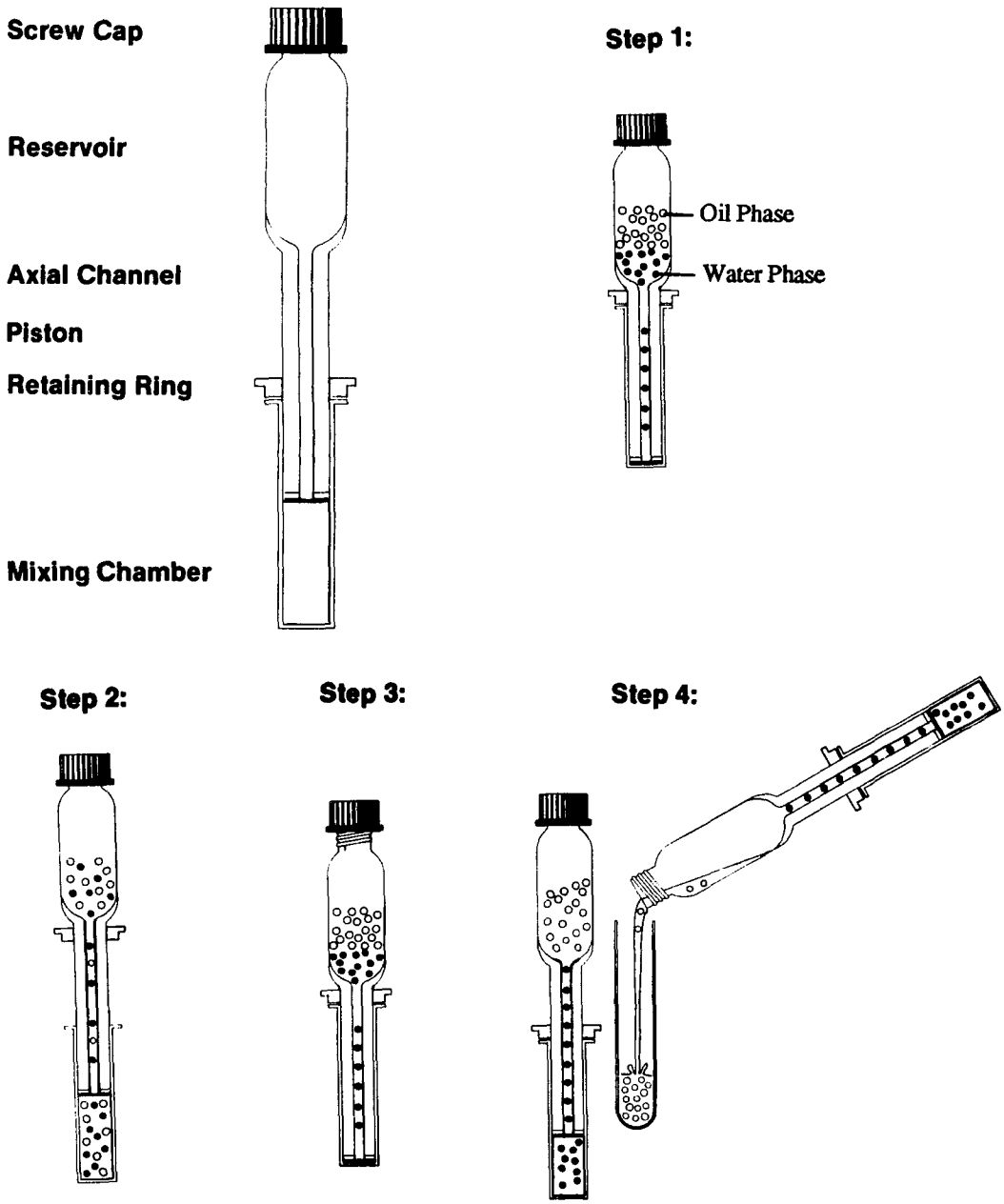

Preparation of Mobile Phase

The mobile phase was prepared by mixing 27% (v/v) acetonitrile (HPLC grade, Baxter Company, Muskegon, MI) and 73% (v/v) 0.1M, pH 2.2 phosphate buffer; 18 µl (0.42 mmol/L) of triethylamine (Sigma Company, St. Louis, MO) was added to improve peak shape, and the mixture was stirred for 10 minutes. The final pH was adjusted to 2.5 with phosphoric acid, if necessary. The mobile phase was then filtered through a 0.45 µm millipore filter (Rainin Company, Woburn, MA) and degassed by sonication (Bransonic Ultrasonic Cleaner, Branson Ultrasonic Corporation, Danbury, CT) for 15 minutes. The mobile phase was continously purged with helium gas to avoid air bubbles.

Preparation of MT-II Stock Solution

The stock solution (1 mg/ml) of MT-II was prepared by dissolving 1 mg MT-II in 1 ml purified water. This solution was refrigerated and was prepared fresh every week.

Melanotan-II Degradation Kinetics

The sample solution (10 µg/ml) was prepared by diluting a stock solution of Melanotan-II with pH 7.0, 0.02 M phosphate buffer solution. The sample solution was stored in an oven at 60°C and was injected onto the HPLC column every 12 hr for up to 144 hr.

Effect of Simulated Gastric Fluid on Stability

The sample solutions (10 μg/ml) were prepared by diluting a stock solution of MT-II with the following solutions:

Test A (Simulated Gastric Fluid as described in the USP XX): (0.2g NaCl + 0.7 ml HCl + 0.32g pepsin) / 100 ml H_2O, pH 1.25

Control B: H_2O, pH 7.05

Control C: (0.2g NaCl + 0.7 ml HCl) / 100 ml H_2O, pH 1.21

Control D: 0.7 ml HCl / 100 ml H_2O, pH 1.20

The sample solutions were than stored at 37°C, and aliquots were taken at suitable time intervals and were directly injected onto the HPLC column for analysis of the amount of intact MT-II remaining.

Effect of Temperature on Stability

The sample solutions (10 μg/ml) were prepared by diluting a stock solution of MT-II in pH 7.0 phosphate buffer (0.01M) and were stored at appropriate temperatures (i.e., 50, 60, and 70°C). Samples were then taken at suitable time intervals and were directly injected onto the HPLC column for analysis of the amount of intact MT-II remaining.

Effect of pH on Stability

All the sample solutions (10 μg/ml) were prepared by diluting a stock solution of MT-II in phosphate buffer solutions at several different pH values. The phosphate buffer

solutions were made by using different mixtures of KH_2PO_4 and K_2HPO_4; 0.1 N HCl or 0.01 M KOH solutions were used to adjust to the desired pH. Low buffer concentration were used to minimize the possible general acid-base catalysis by the buffer species. The concentration of the total phosphate buffer was 0.02M. Ionic strength was adjusted to a constant μ=0.15 by adding potassium chloride. The sample solutions were put into polypropylene tubes and were placed in a constant temperature oven at 60°C. The amount of MT-II remaining after certain time intervals was analyzed by the HPLC method.

Effect of Buffer Concentration on Stability

Buffer solutions were made by mixing the same proportions (but different amounts) of KH_2PO_4 and K_2HPO_4, to produce different buffer concentrations (0.02M, 0.10M, 0.50M). KCl was added to adjust each solution to a constant ionic strength (μ=1.5). Each solution pH was adjusted to pH 9.11 with 0.01 M KOH. The sample solutions (10 μg/ml) with different buffer concentrations were put into polypropylene tubes and were placed in a constant temperature oven at 60°C. The amount of MT-II remaining after certain time intervals was analyzed by the HPLC method.

Effect of Ionic Strength on Stability

All the sample solutions (10 μg/ml) were prepared by diluting the stock solution of MT-II with phosphate buffer solution of several different ionic strengths (0.15, 0.25, 0.50, 0.75, 1.00, 1.25, 1.50) but the same pH values (pH 9.11) and same total buffer concentrations. The different ionic strengths were made by adding different amounts of

potassium chloride. The sample solutions were put into polypropylene tubes and placed in a constant temperature oven maintained at 60°C. The amount of MT-II remaining after certain time intervals was analyzed by the HPLC method.

pKa Determination by Potentiometric Titration

The sample solution was made by adding 4 mg of MT-II into 3 ml of H_2O. The sample solution was titrated with 0.01 M KOH. Nitrogen gas was instilled into the sample solution during the whole titration to avoid CO_2 formation. The pH values of the sample solutions were read by a pH meter during the titration.

pKa Determination by UV Spectrophotometric Method

The absorbance of sample solutions (10 μg/ml) with different pH values was read at 214 nm on a recording spectrophotometer (Model 40, Beckman Instruments, Fullerton, CA). To avoid any possible precipitation of MT-II, especially at high pH values, each solution was measured immediately after preparation.

Partition Coefficients

Each Mixxor separatory cylinder was coated with 100 μl of silicone (Silicote, Sigma Company) to minimize the adsorption of MT-II to the glass surface. Since silicone coating cannot totally prevent the adsorption, a control experiment was performed to correct for the adsorption of the peptide. One ml of MT-II sample solution (12 μg/ml in pH 7.35

phosphate buffer) and 1 ml octanol were added to the graduated glass mixing reservoir. A control experiment used 2 ml MT-II sample solution. With the holder-spacer in the upper position of the separatory cylinder, the piston was pushed fully into the mixing reservoir in an up and down movement, 15, 30, 50, 60, 70, and 80 times, in order to determine the appropriate mixing times to obtain equilibrium. The mixed liquids were then allowed to separate into an upper and lower phase. The upper layer (oil phase) was decanted. The lower layer (water phase) was injected (70 µl) onto the HPLC system to determine the amount of MT-II left in the water phase.

Sample solutions of pH 4.57, pH 7.35, and pH 12.20 were then tested with both octanol and isooctane as the oil phase using the procedures described previously using 70 oscillations of the Mixxor. Each partition coefficient was determined in triplicate. The partition coefficients (P.C.) were then calculated as follows:

$$\text{P.C.} = \frac{\text{Concentration in control - Concentration in buffer phase}}{\text{Concentration in buffer phase}} \qquad \text{Eq.(12)}$$

CHAPTER IV
RESULTS AND DISCUSSION

HPLC Assay

As shown in Figure 4, Melanotan-II was eluted with a retention time of about 5.7 mins. The peak was well resolved from other peaks. Calibration curves showed a good linear correlation ($r > 0.999$).

Melanotan-II Degradation Kinetics

The degradation of MT-II in pH 7.0, 0.02 M phosphate buffer solution followed apparent first-order kinetics (Table1; Figures 5 and 6). The apparent first-order rate constant (Kobs) was found to be 6.87×10^{-3} hr^{-1}. This value represents the slope of the line of best-fit of the data shown in Figure 5 obtained by least-squares linear regression of the logarithm (to the base *e*) of the concentration versus time data. The value of Kobs was then substituted into the first-order rate expression, i.e., $C_t = C_0 e^{-Kt}$ to obtain the "first-order fit" line shown in Figure 6. The excellent fit of the data to the model indicates that a first-order process is responsible for the degradation of MT-II.

Effect of Simulated Gastric Fluid on Stability

The degradation of MT-II by simulated gastric juice is shown in Figure 7 and Table 2. It appears that MT-II is relatively stable in hydrochloric acid. Compared to the other control solutions, pepsin caused more degradation than other components of simulated

gastric fluid. However, even in simulated gastric fluid, more than 90% of undegraded MT-II would pass into the intestine within the typical stomach retention and emptying time since the gastric emptying half-time ($T_{1/2}$ GE) in normal subjects ranges from 25-75 min (Theodorakis et al., 1980). Our results here partially confirm a previous report which indicated that MT-II is relatively stable to degradation by some degradative enzymes present in the gastrointestinal tract, i.e., trypsin, chymotrypsin, and pepsin (Hadley et al., 1989).

Effect of Temperature on Stability

The effect of temperature on the degradation of MT-II was investigated by measuring the rate of degradation in water at 50, 60, and 70°C. The values of Kobs at the different temperature are shown in Table 3 and Figure 8. The Arrhenius plot for the degradation of MT-II at pH 7.0 and constant ionic strength was linear. On the basis of these data, the apparent energy of activation (Ea) was calculated from the slope of the Arrhenius plot (Figure 9) and was determined to be 7.53 Kcal/mole. The preexponetial constant (A) was calculated from the intercept to be 1301.4 hr^{-1}. The enthalpy ($\Delta H^{\ddagger}$) at different temperatures was calculated by the following equation:

$$\Delta H^{\ddagger} = Ea - RT \qquad \text{Eq.(13)}$$

and the shelf life (t_{90}) was calculated by

$$t_{90} = 0.105/Kobs \qquad \text{Eq.(14)}$$

The parameters at 25°C were found by extrapolation : Kobs = 0.0039 hr^{-1}, $\Delta H^{\ddagger}$ = 6.94 Kcal/mole, and t_{90} = 26.92 hr.

Effect of pH on Stability

The apparent first-order degradation rate constants Kobs at different pH values are shown in Table 4. Figure 10 shows the pH-rate profile of MT-II.

The rate of degradation of MT-II at various pH values followed apparent first-order kinetics over the time course of the studies. From the pH-rate profile shown in Figure 10, the pH of optimum stability was estimated to be 5.0. The parameters of equation 3 were found from this pH-rate profile. The slope at low pH values is -0.102 (standard error; S.E. = 0.000 from two points), and the slope at high pH is 0.127 (S.E.= 0.020), therefore, the order with respect to hydrogen ion is 0.102; the order with respect to hydroxyl ion is 0.127. The other rate data were fitted by nonlinear least-squares (Metzler and Weiner, 1986) analysis by fixing n at 0.102 and m at 0.127 and using a three-parameter fit to estimate: K_{H^+}, K_O, K_{OH^-}. The best fit provided values of K_{H^+} = 0.015 (S.E. = 0.004), K_O = -0.003 (S.E. = 0.002), and K_{OH^-} = 0.047 (S.E. = 0.006). Therefore, the rate equation can be written as follow:

$$K_{obs} = 0.015\,[H^+]^{0.102} + 0.047\,[OH^-]^{0.127} \qquad \text{Eq.(15)}$$

From these data, the following conclusions can be made:

1. The reaction is not specific acid-catalysis by hydrogen ion or specific base -catalysis by hydroxyl ion since the slope in either pH region is not -1 or +1. This indicates that the compound degrades by several different pathways, each with its own pH dependence and true catalytic coefficient,
2. The uncatalyzed term (water) does not play a role in the degradation of MT-II,
3. The hydroxyl ion has more effect than hydrogen ion in the degradation of MT-II.

Effect of Buffer Concentration on Stability

The log percentage remaining versus time is shown in Figure 11, and Kobs for degradation of MT-II is displayed in Table 5. These data show that the degradation rate of MT-II increases with increasing buffer concentration.

Melanotan-II acetate may exist as the neutral, monoacidic or diacidic cationic species depending on the pH of the reaction medium. Therefore, in aqueous media, the following equilibrium expressions may be writen for MT-II:

$$BH^{2+} \rightleftharpoons BH^{+} + H^{+} \qquad \text{Eq.(16)}$$

$$BH^{+} \rightleftharpoons B + H^{+} \qquad \text{Eq.(17)}$$

where B, BH^{+}, and BH^{2+} denote the neutral, monoacidic and diacidic cationic species, respectively. The effect of buffer concentration on the rate of degradation was studied at a constant pH of 9.11. At this pH, the equilibrium represented by Eq.(17) predominates, since pH is much larger than pKa1. Therefore, it can be assumed that either BH^{+} or B can undergo degradation. The following kinetic schemes may then be written:

BH^{+} ------> Products Eq.(18), or

B ------> Products Eq.(19)

In the above equations, the two forms of MT-II can react with hydroxyl ion, hydrogen ion, or the phosphate buffer species to form the degradation products. Another experiment showed that ionic strength had no effect on the rate of degradation of MT-II. Therefore, the

reaction of both charged species can be eliminated from consideration; one of the reactants must be a neutral species. Since hydroxyl ion, hydrogen ion, and the phosphate buffer species are all charged species, it follows that the uncharged reactant has to be the neutral form (B) of MT-II. Therefore, the reaction represented by Eq(18) can be assumed not to occur. From Eq(19), the generalized rate equation may be written as follows:

$$d(\text{Products})/dt = K_{obs}[B] \qquad \text{Eq.(20)}$$

Kobs can be decomposed into individual rate equations for specific acid/base and general acid/base catalysis. Hence, the general overall observed rate constant Kobs may be written as follow:

$$K_{obs} = K_o + K_1[H^+] + K_2[OH^-] + K_3[H_2PO_4^-] + K_4[HPO_4^=] \qquad \text{Eq.(21)}$$

The results show that the contribution of acid/base catalysis to the overall rate of degradation is highly significant. At the experimental pH 9.11, the predominant phosphate buffer species is $HPO_4^=$ and the hydrogen ion concentration is very low. Therefore, the overall rate equation can be simplified to:

$$K_{obs} = K_o + K_2[OH^-] + K_4[HPO_4^=] \qquad \text{Eq.(22)}$$

Effect of Ionic Strength on Stability

The Kobs at different ionic strengths are shown in Table 6. When log Kobs is plotted versus $\sqrt{\mu}/(1+\sqrt{\mu})$, the slope shows the effect of ionic strength (salt effect) on degradation (Figure 12). Correlation and regression analysis indicated that no significant correlation existed between log Kobs and $\sqrt{\mu}/(1+\sqrt{\mu})$, and the slope of the plot did not show any significant difference from zero (p= 0.983). Therefore, the log Kobs was independent of the ionic strength (μ). In other words, the kinetic salt effect on the degradation kinetics of MT-II at pH 9.11 was interpreted to be negligible.

pKa Values

From the chemical structure of MT-II, we can assume that the possible dissociating sites are histidine and arginine. The pKa of His is about 6-7, the pKa of Arg is about 11-13. Therefore, we can predict that the pKa of MT-II may be within those two ranges.

pKa1 Determination by Potentiomteric Method

The results of the potentiometric titration method are shown in Table 7 and Figure 13. We can determine the pKa1 by linearizing a segment of the titration curve using the modified Gran function method. (Seymour et al., 1977) The reactions during the titration can be illustrated by the following equations:

$$CH_3COOH \rightleftharpoons H^+ + CH_3COO^- \qquad \text{Eq.(23)}$$

$$BH_2^{2+} \rightleftharpoons H^+ + BH^+ \qquad \text{Eq.(24)}$$

$$BH^+ \rightleftharpoons H^+ + B \qquad \text{Eq.(25)}$$

$$KOH \longrightarrow K^+ + OH^- \qquad \text{Eq.(26)}$$

BH_2^{2+} and BH^+ are the diacetate and monoacetate forms of MT-II, respectively. Stoichiometrically, 1 mole of MT-II diacetate can release 2 moles of acetic acid, therefore, the concentration of acetic acid is twice the concentration of MT-II diacetate. If Ca represents the concentration of MT-II diacetate, and Cb represents the concentration of acetic acid, then:

$$Cb = 2\,Ca \qquad \text{Eq. (27)}$$

The concentration of each ionic species can be written as the following equations:

$$[CH_3COO^-] = \frac{2CaK_A}{[H^+] + K_A} \qquad \text{Eq.(28)}$$

where K_A represents the ionization constant of acetic acid (1.74×10^{-5}).

$$[BH_2^{2+}] = \frac{[H^+]^2Ca}{[H^+]^2 + Ka_1[H^+] + Ka_1Ka_2} \qquad \text{Eq.(29)}$$

$$[BH^+] = \frac{Ka_1[H^+]Ca}{[H^+]^2 + Ka_1[H^+] + Ka_1Ka_2} \qquad \text{Eq.(30)}$$

where Ka_1 and Ka_2 are the first and second ionization constants of MT-II.

$$[K+] = \frac{V_{KOH} \times M_{KOH}}{V_{KOH} + V_o} \qquad \text{Eq.(31)}$$

where V_{KOH} and Vo denote the volumes of potassium hydroxide and the initial volume of MT-II sample solution, respectively, and M_{KOH} is the molarity of potassium hydroxide.

$$[OH^-] = \frac{K_w}{[H^+]} \qquad \text{Eq.(32)}$$

where K_w is the ion-product of water.

The electroneutrality condition is expressed by the equation:

$$[CH_3COO^-] + [OH^-] = [H^+] + [K^+] + 2[BH_2^{2+}] + [BH^+] \qquad \text{Eq.(33)}$$

Substituting equations (28)-(32) into equation (33), the following result is obtained:

$$1/Ca\ \{(2K_ACa / [H^+] + K_A) + (Kw/[H^+]) - (V_{KOH} \times M_{KOH} / V_{KOH} + Vo) - [H^+]\}$$
$$= \frac{2[H^+]^2 + Ka_1[H^+]}{[H^+]^2 + Ka_1[H^+] + Ka_1Ka_2} \qquad \text{Eq.(34)}$$

The left-hand side represents the experimentally observable parameters and therefore can be simplified by a symbol F.

$$F = 1/Ca\{(2K_ACa / [H^+] + K_A) + (Kw/[H^+]) - (V_{KOH} \times M_{KOH} / V_{KOH} + Vo) - [H^+]\} \qquad \text{Eq.(35)}$$

Therefore:

$$F = \frac{2[H^+]^2 + Ka_1[H^+]}{[H^+]^2 + Ka_1[H^+] + Ka_1Ka_2} \qquad \text{Eq.(36)}$$

The linear transformation of equation(33) can be written as follows:

$$[H^+]^2(2-F)/F = Ka_1 \times [H^+](F-1)/F + Ka_1Ka_2 \qquad \text{Eq.(37)}$$

The various volumes of titrant (KOH) and the hydrogen-ion concentrations $[H^+]$ at corresponding pH values (shown in Table 7) were substituted into equation 35 and several F values were calculated. The various F values and the corresponding hydrogen-ion concentrations were then fitted to equation 37 using least-squares linear regression analysis. The equation 37 showed linear correlation between $[H^+]^2(2-F)/F$ and $[H^+](F-1)/F$. The correlation coefficient was 0.99 and the slope, which is the first ionization constant (Ka_1), was 2.88×10^{-7} and the pKa_1 value was calculated to be 6.54, which corresponds to the histidine residue.

By this method, the pKa_1 was determined. However, there was no discrete inflection point for the second titratable group, therefore, Ka_2 could not be determined accurately by this method even though the Ka_2 might be calculated from the intercept of equation 37. Carbon dioxide interfered with the measurements at high pH since CO_2 reacted with the OH^- and caused a buffer like effect, thus masking the inflection point.

pKa2 Determinarion by UV Spectrophotometric Method

The spectrophotometric data read at 214 nm (Table 8) were fitted to the following form of the Henderson-Hasselbalch equation using a non-linear regression program (Metzler and Weiner, 1986):

$$A_T = [Au + Ai \cdot 10^{(pKa - pH)}]/[1 + 10^{(pKa - pH)}] \qquad \text{Eq.(38)}$$

where A_T is the total absorbance, Au is the absorbance of unionized form, and Ai is the absorbance of the ionized form. The pKa2 was computed to be 11.72 which corresponds to the arginine residue (Figure 14).

Knowledge of the ionization constants will be very useful in determining the proportions of the different ionic and nonionic species of MT-II present at a given pH. The percentage of the various forms of Melanotan-II at different pH values (shown in Figure 15) can be calculated by substituting the values of K_{a1} and K_{a2} into equation 29 and 30 for BH_2^{2+} and BH^+, respectively. The fraction of MT-II in the unionized [B] form is calculated by substituting $K_{a1} \times K_{a2}$ as the numerator in equations 29 or 30. This information will, in turn, help us to predict the solubility and kinetic behavior, and the partitioning of MT-II into biological membranes at various pH values.

Partition Coefficients

The results of the equilibration experiments are shown in Figure 16 and indicate that 70 oscillations of the Mixxor apparatus were adequate to achieve equilibration of MT-II between the two phases.

The results of the partition coefficient experiments were expressed using the following equations:

Δ log P.C. = log P.C. (octanol) - log P.C. (isooctane), or

Δ log P.C. = log (P.C. octanol / P.C. isooctane)

The Δ log P.C. value has been reported to be a measure of the hydrogen-bonding potential of the peptide and thus a direct measure of the "desolvation energy" of the peptide

which is, in turn, an important measure of the absorption potential of the peptide across biological membranes such as those in the gastrointestinal tract. The results of the MT-II partition coefficient determinations are shown in Table 9 and Figure 17. These data were consistent with the results of the pKa determinations. When the sample solutions were at pH 12.20, the MT-II was almost completely in its unionized [B] form, so it has a high partition into the oil phase. When the sample solutions were at pH 7.35, the MT-II exists in both of its ionized forms, mostly [BH^+], so the partitioning into the oil phase was lower. When the sample solutions were at pH 4.57, the MT-II was almost completely in its [BH_2^{2+}] form, so it had a low partition into the oil phase. These results indicate that the gastrointestinal absorption potential of Melanotan-II is very good.

Figure 4.

HPLC Results for MT-II

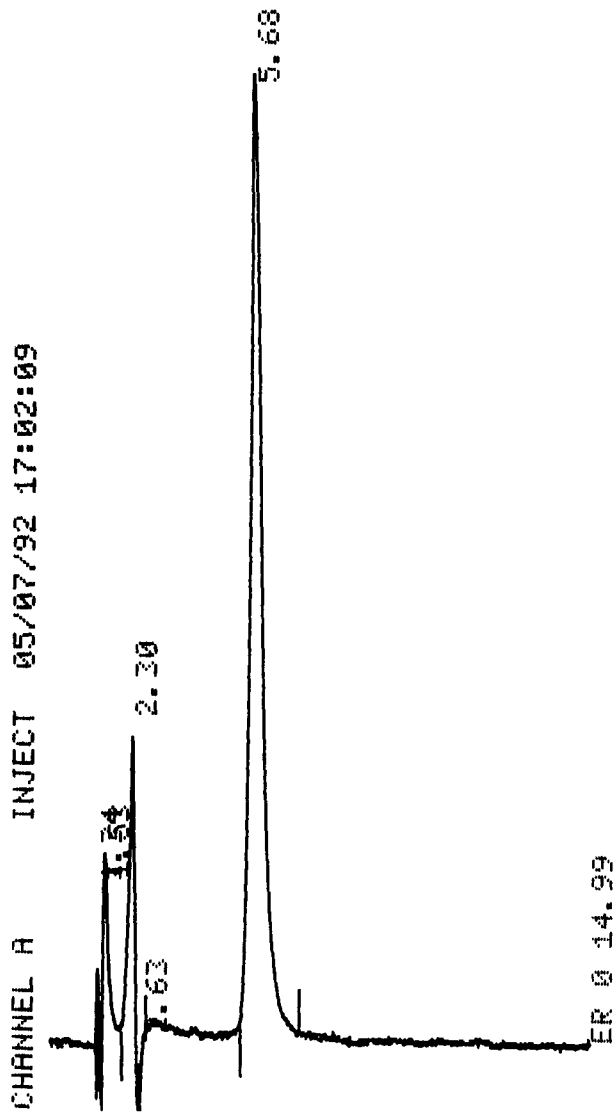

Table 1.

MT-II Degradation Kinetics in pH 7.0, 0.02 M Phosphate Buffer Solution

Time (hr)	% Remaining	ln % Remaining
0	100.00	4.605
24	82.02	4.407
36	79.30	4.373
48	70.84	4.260
60	63.16	4.146
72	62.10	4.129
84	55.11	4.009
96	51.34	3.938
108	48.81	3.888
120	42.78	3.756
132	40.48	3.701
144	40.78	3.708

Figure 5.

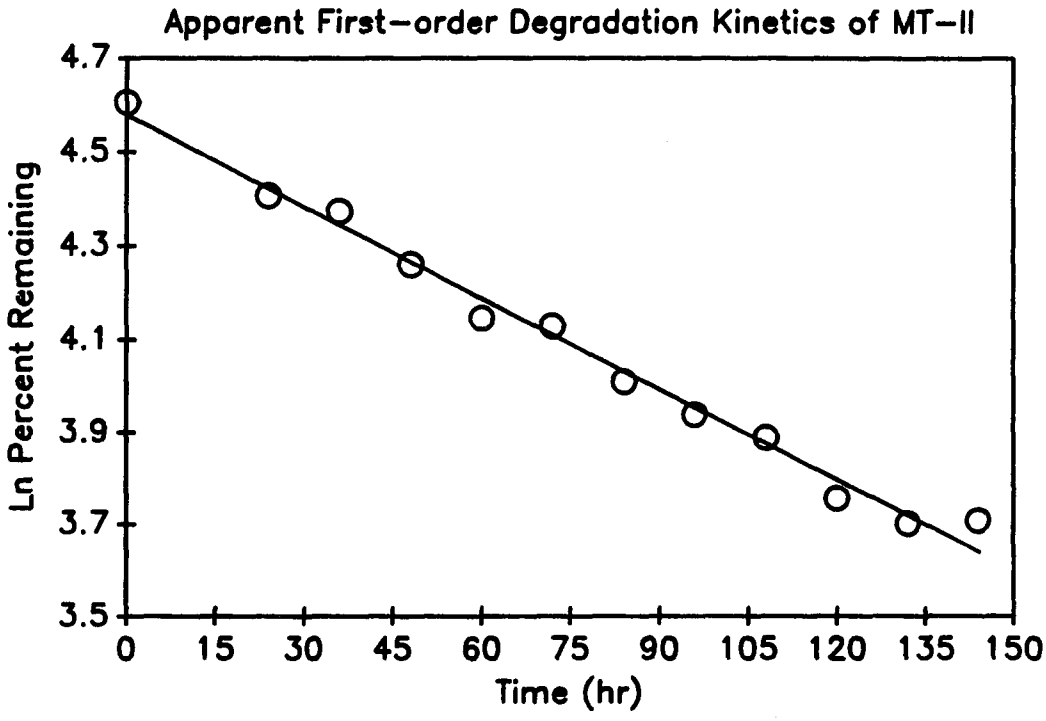
Apparent First-order Degradation Kinetics of MT-II
Ln Percent Remaining
4.7
4.5
4.3
4.1
3.9
3.7
3.5
0
15
30
45
60
75
90
105
120
135
150
Time (hr)

Figure 6.

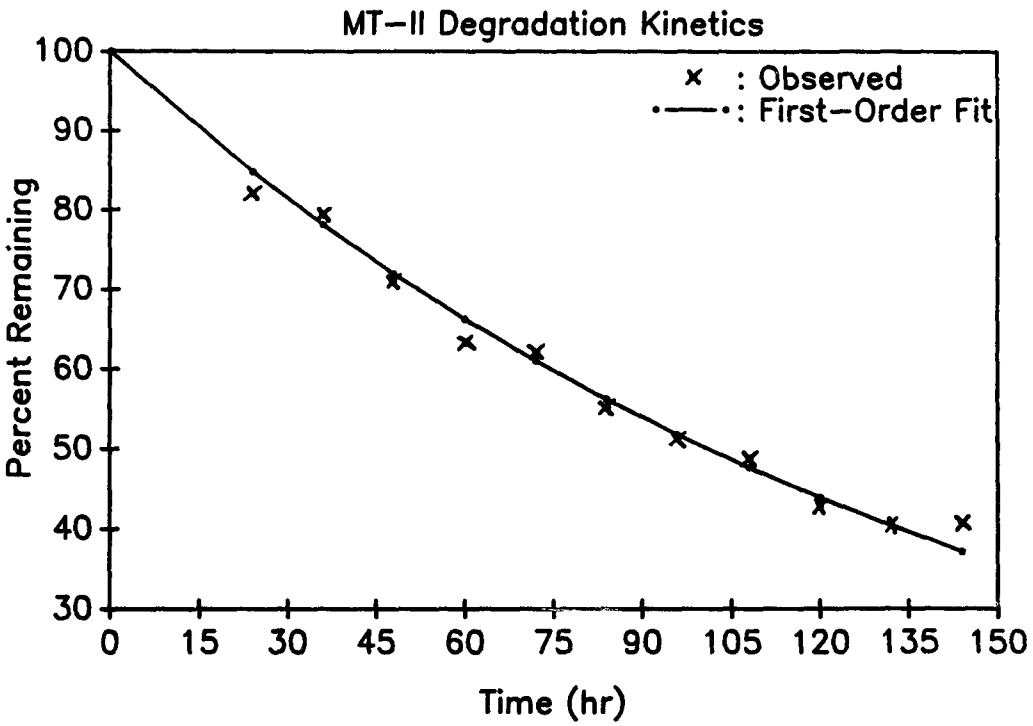
MT–II Degradation Kinetics
× : Observed
•——•: First–Order Fit
Percent Remaining
100
90
80
70
60
50
40
30
0
15
30
45
60
75
90
105
120
135
150
Time (hr)

Table 2.

Percentage of MT-II Remaining in Simulated Gastric Fluid and in Control Solutions

Time (hr)	A	B	C	D
0	100.00	100.00	100.00	100.00
1	99.99	—	—	—
2	98.89	—	—	—
4	93.75	103.13	94.46	99.92
6	92.97	—	—	—
8	89.19	99.01	96.62	97.98
12	84.82	97.01	89.04	—
13	—	—	—	96.79
20	76.68	—	—	—
24	73.51	96.07	98.88	100.53
36	69.22	—	—	—
48	60.33	—	—	—

A: Simulated Gastric Fluid
B: Distilled Water
C: HCl + NaCl / Distilled Water
D: HCl / Distilled Water

Figure 7.

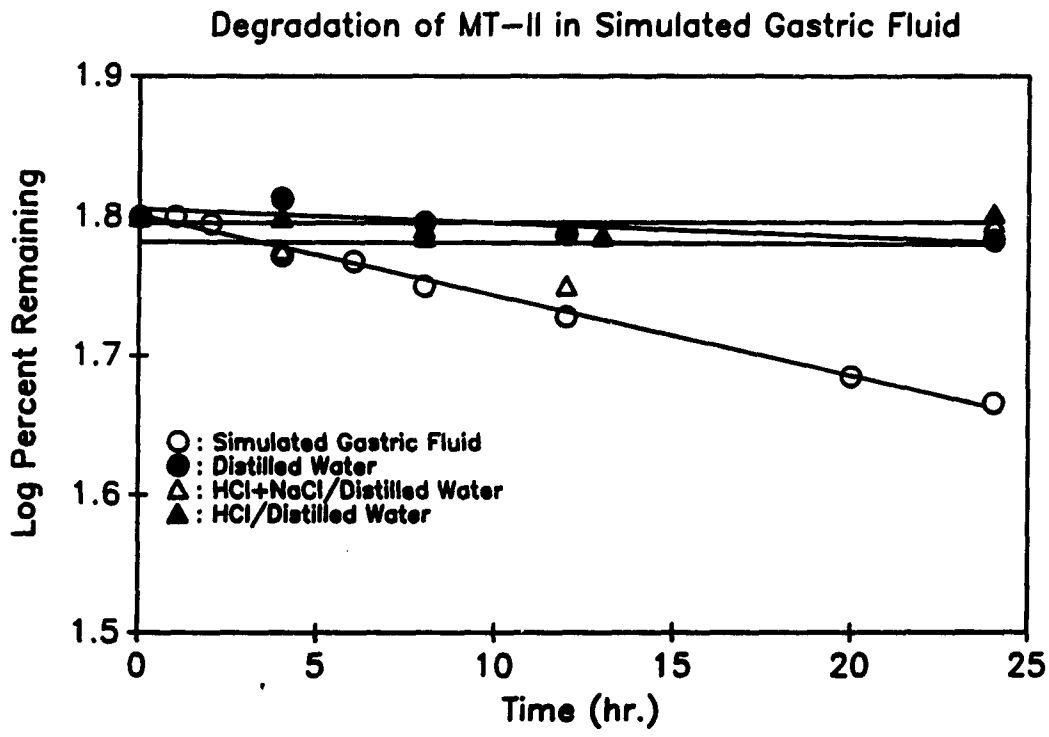
Degradation of MT–II in Simulated Gastric Fluid
Log Percent Remaining
1.9
1.8
1.7
1.6
1.5
0
5
10
15
20
25
Time (hr.)
○ : Simulated Gastric Fluid
● : Distilled Water
△ : HCl+NaCl/Distilled Water
▲ : HCl/Distilled Water

Table 3

Percentage of MT-II Remaining at Different Temperatures

Time(hr)	50°C	60°C	70°C
0	100.00	100.00	100.00
2	101.33	97.32	94.79
4	96.54	94.69	90.78
6	96.19	91.62	87.15
8	93.81	89.04	84.83
10	—	85.52	81.23
12	89.28	—	—
Kobs(hr^{-1})	0.0102	0.0155	0.0202
t_{90}(hr)	10.29	6.77	5.20
$\Delta H^{\ddagger}$(Kcal/mole)	6.89	6.87	6.85

Figure 8.

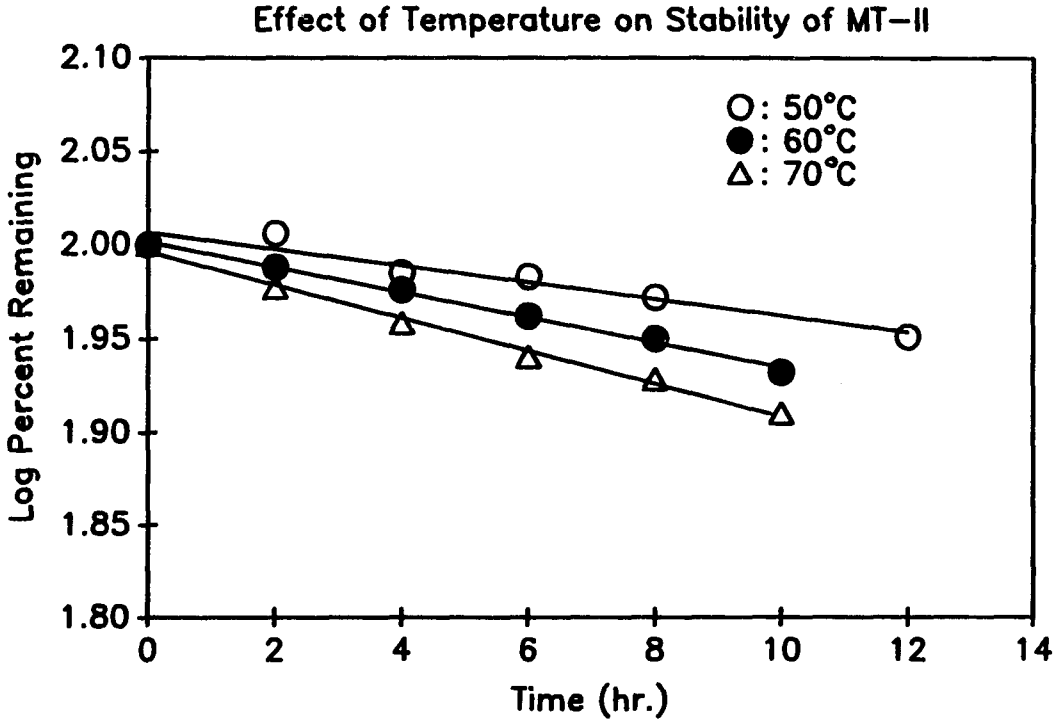
Effect of Temperature on Stability of MT-II
Log Percent Remaining
2.10
2.05
2.00
1.95
1.90
1.85
1.80
O: 50°C
●: 60°C
△: 70°C
0
2
4
6
8
10
12
14
Time (hr.)

Figure 9.

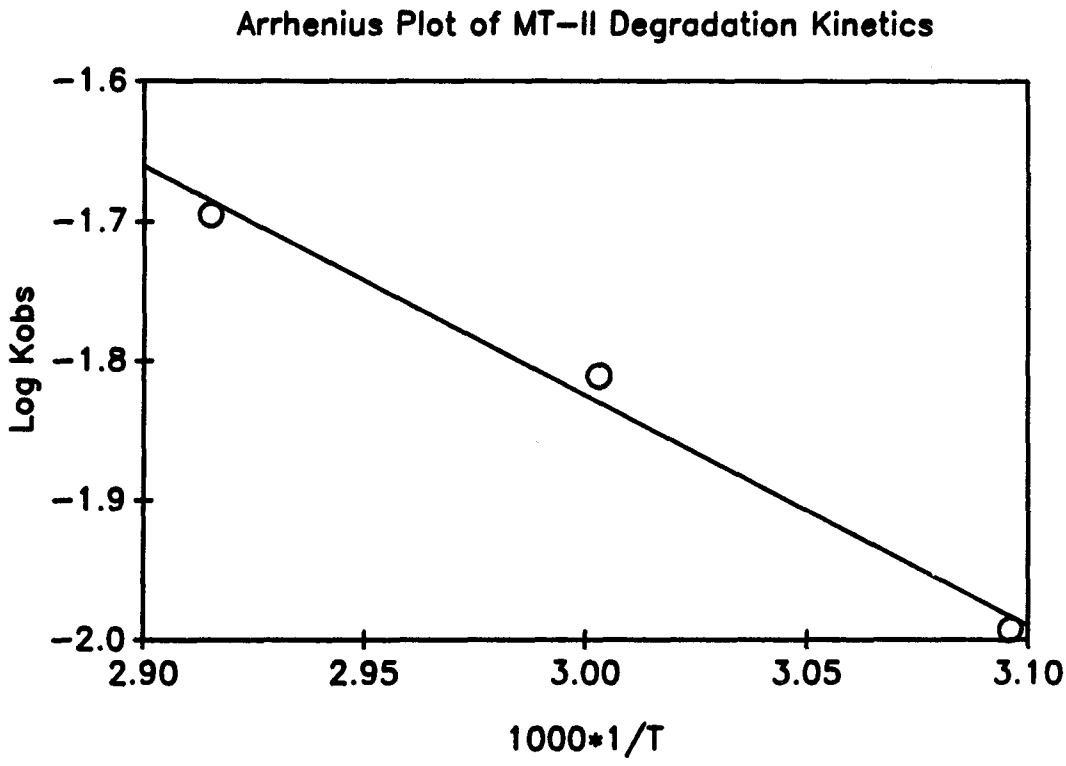
Arrhenius Plot of MT-II Degradation Kinetics
Log Kobs
-1.6
-1.7
-1.8
-1.9
-2.0
2.90
2.95
3.00
3.05
3.10
1000*1/T

Table 4

Percentage of MT-II Remaining at Different pH Values

Time (hr)	pH 2.78	pH 3.83	pH 5.47	pH 7.45	pH 8.25	pH 8.75	pH 9.13
0	100.00	100.00	100.00	100.00	100.00	100.00	100.00
1	—	—	—	100.11	—	—	—
2	102.07	99.93	—	99.92	92.16	—	96.49
2.5	—	—	99.31	—	—	—	—
4	98.75	98.76	99.74	96.03	92.11	99.11	95.22
6	96.63	95.81	—	94.20	90.60	94.09	93.18
6.5	—	—	98.45	—	—	—	—
8	—	96.32	—	—	89.92	88.77	88.38
10	—	94.27	—	92.46	87.94	88.18	88.91
10.5	—	—	95.65	—	—	—	—
11	—	—	—	—	—	86.58	—
12	94.68	—	—	—	—	—	—
14	89.16	—	—	—	—	—	—
Kobs(hr^{-1})	0.0080	0.0062	0.0054	0.0090	0.0105	0.0146	0.0158

Figure 10.

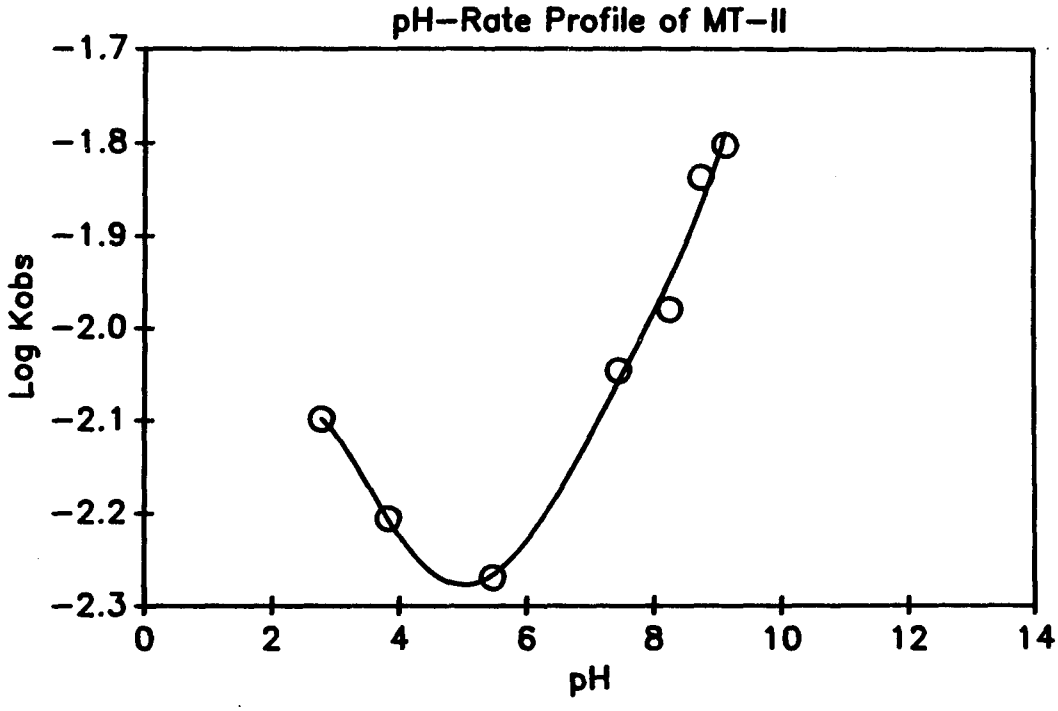
pH–Rate Profile of MT–II
Log Kobs
−1.7
−1.8
−1.9
−2.0
−2.1
−2.2
−2.3
0
2
4
6
8
10
12
14
pH

Table 5

MT-II Degradation in Phosphate Buffer Solutions of Different Concentrations

Time (hr)	0.02M	0.10M	0.50M
0	100.00	100.00	100.00
2	—	97.58	93.79
3	97.24	—	—
4	—	93.53	87.07
5	95.48	—	—
6	94.14	91.42	84.46
8	92.65	85.33	75.21
9	—	83.88	—
10	90.48	—	67.23
Kobs(hr^{-1})	0.0100	0.0200	0.0383

Figure 11.

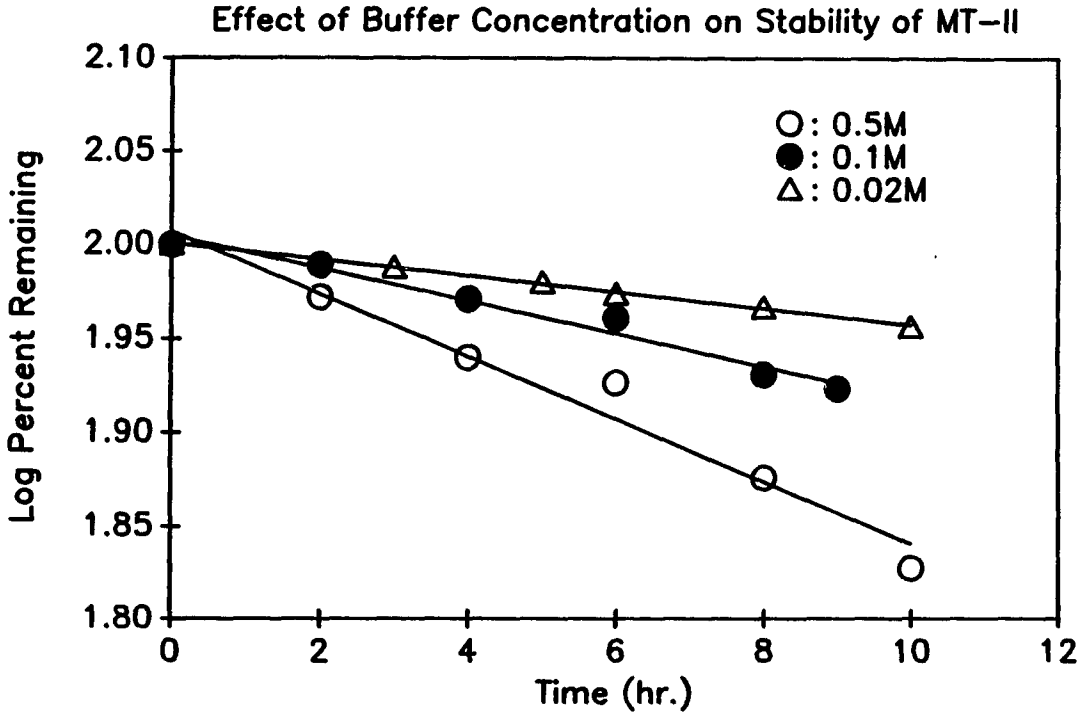
Effect of Buffer Concentration on Stability of MT-II
Log Percent Remaining
2.10
2.05
2.00
1.95
1.90
1.85
1.80
O: 0.5M
●: 0.1M
Δ: 0.02M
0
2
4
6
8
10
12
Time (hr.)

Table 6.

MT-II Degradation in Phosphate Buffer Solutions of Different Ionic Strength

Time (hr)	μ=0.15	μ=0.25	μ=0.50	μ=0.75	μ=1.00	μ=1.25	μ=1.50
0	100.00	100.00	100.00	100.00	100.00	100.00	100.00
2	—	—	96.90	95.97	92.66	94.97	—
3	—	—	—	—	—	—	97.24
4	99.11	95.64	—	91.42	—	—	—
5	—	—	—	—	—	—	95.48
6	94.09	—	88.66	87.85	88.13	—	94.14
7	—	93.05	—	—	—	91.86	—
8	88.77	92.28	87.63	83.77	—	86.82	94.14
10	88.18	88.20	83.60	81.39	80.57	84.69	90.48
11	86.58	85.59	—	—	—	—	—
12	—	—	78.73	—	76.03	79.11	—
14	—	—	—	—	73.66	—	—
Kobs(hr^{-1})	0.0146	0.0133	0.0180	0.0211	0.0211	0.0176	0.0100

Figure 12.

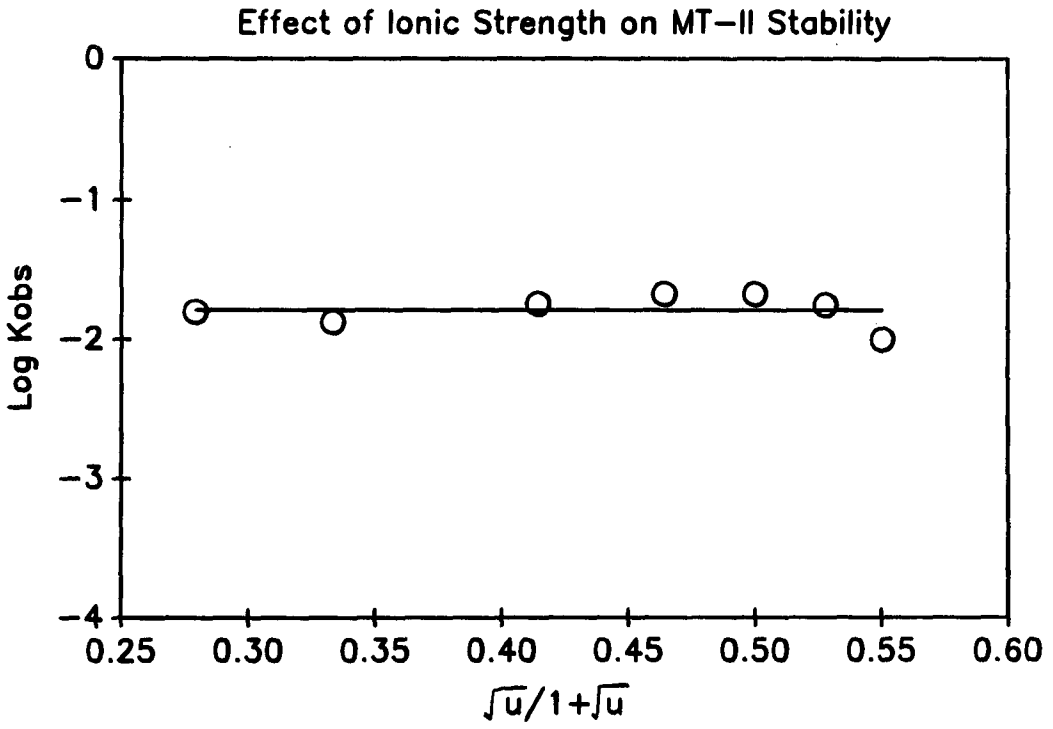
Effect of Ionic Strength on MT-II Stability
Log Kobs
0
-1
-2
-3
-4
0.25
0.30
0.35
0.40
0.45
0.50
0.55
0.60
√u/1+√u

Table 7.

MT-II (0.001M) Titration Data with KOH (0.01M)

Vol. of KOH (ml)	pH	Vol. of KOH (ml)	pH	Vol. of KOH (ml)	pH
0.00	3.73	0.52	8.66	1.04	10.70
0.02	3.88	0.54	9.01	1.06	10.73
0.04	4.06	0.56	9.26	1.08	10.75
0.06	4.32	0.58	9.47	1.10	10.78
0.08	4.62	0.60	9.61	1.12	10.80
0.10	4.95	0.62	9.73	1.14	10.82
0.12	5.24	0.64	9.82	1.16	10.84
0.14	5.47	0.66	9.87	1.18	10.86
0.16	5.63	0.68	9.97	1.20	10.88
0.18	5.79	0.70	10.04	1.22	10.90
0.20	5.90	0.72	10.08	1.24	10.91
0.22	5.97	0.74	10.13	1.26	10.92
0.24	6.02	0.76	10.17	1.28	10.94
0.26	6.11	0.78	10.21	1.30	10.95
0.28	6.23	0.80	10.24	1.32	10.96
0.30	6.32	0.82	10.27	1.34	10.98
0.32	6.42	0.84	10.29	1.36	10.99
0.34	6.53	0.86	10.35	1.38	11.00
0.36	6.63	0.88	10.40	1.40	11.01
0.38	6.75	0.90	10.45	1.42	11.02
0.40	6.87	0.92	10.49	1.44	11.02
0.42	7.00	0.94	10.53	1.48	11.04
0.44	7.16	0.96	10.57	1.56	11.07
0.46	7.34	0.98	10.61	1.66	11.11
0.48	7.63	1.00	10.64	1.72	11.13
0.50	8.07	1.02	10.67		

Figure 13.

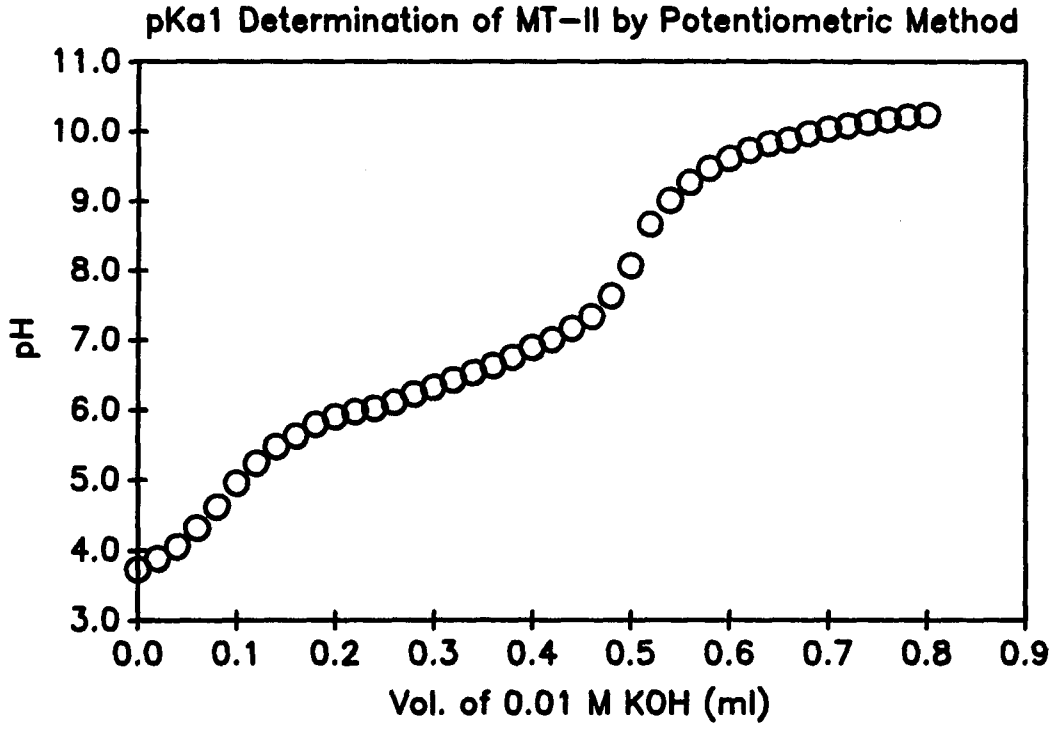
pKa1 Determination of MT-II by Potentiometric Method
11.0
10.0
9.0
8.0
7.0
6.0
5.0
4.0
3.0
pH
0.0
0.1
0.2
0.3
0.4
0.5
0.6
0.7
0.8
0.9
Vol. of 0.01 M KOH (ml)

Table 8.

UV Absorbance of MT-II at Different pH Values

pH	Absorbance
13.171	0.120
12.981	0.120
12.375	0.132
12.084	0.158
11.410	0.267
10.382	0.339
8.786	0.348

Figure 14.

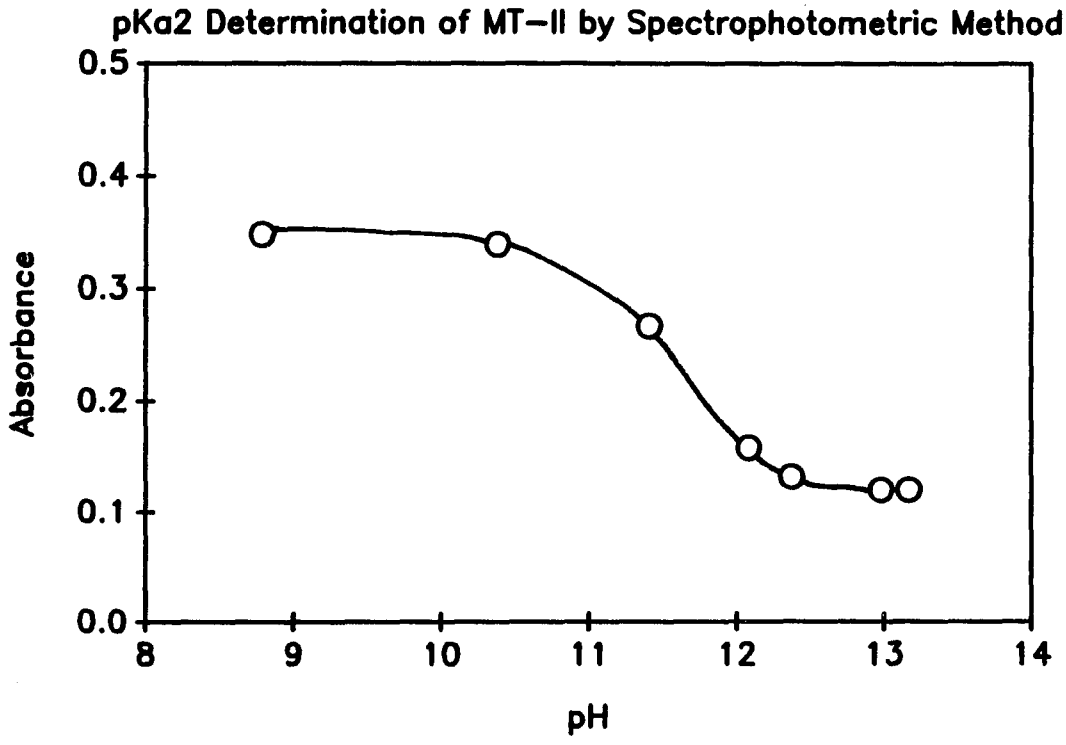
pKa2 Determination of MT–II by Spectrophotometric Method
Absorbance
0.5
0.4
0.3
0.2
0.1
0.0
8
9
10
11
12
13
14
pH

Figure 15.

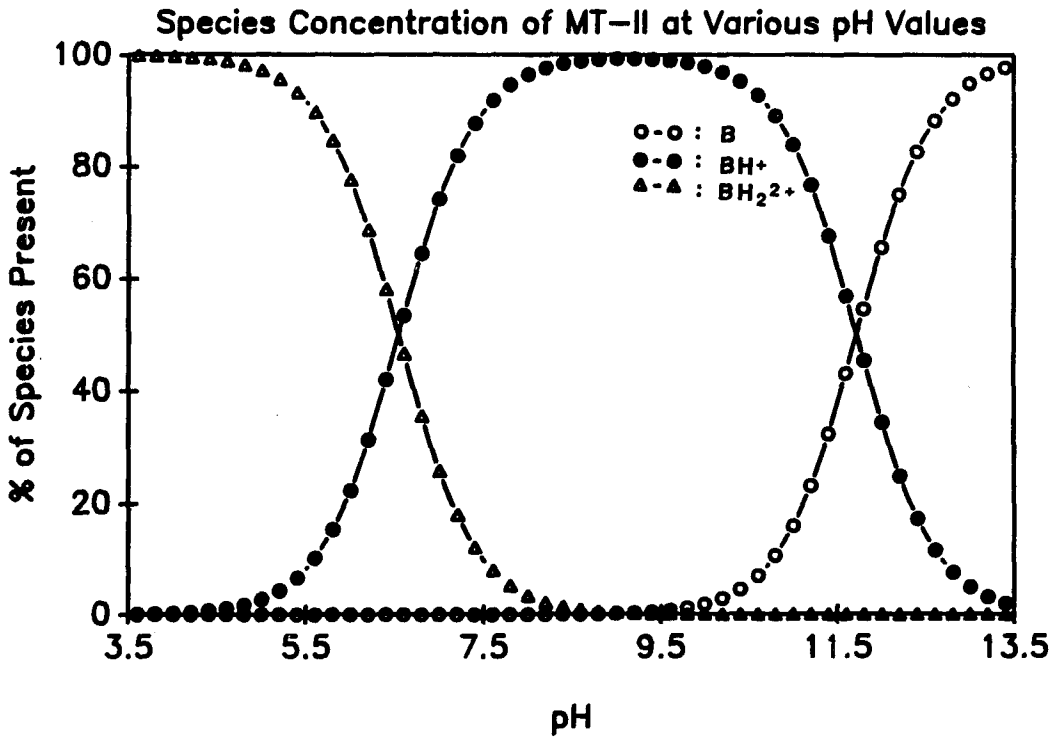
Species Concentration of MT–II at Various pH Values
% of Species Present
100
80
60
40
20
0
3.5
5.5
7.5
9.5
11.5
13.5
pH
o-o : B
●-● : BH+
▲-▲ : BH2 2+

Figure 16.

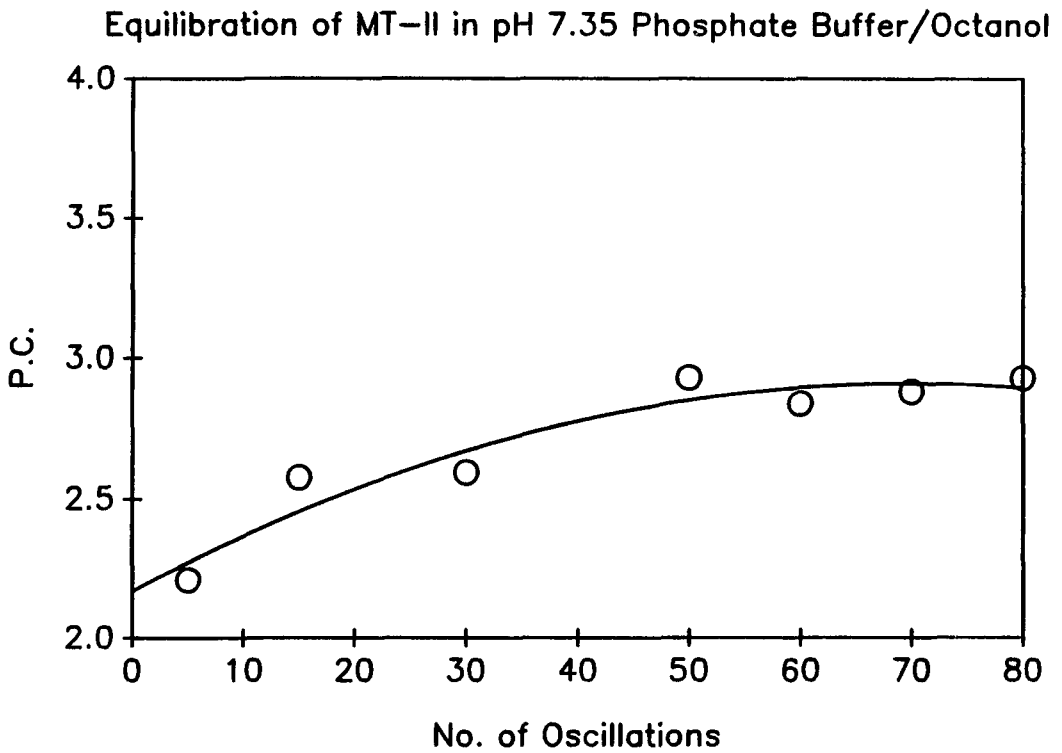
Equilibration of MT–II in pH 7.35 Phosphate Buffer/Octanol
P.C.
4.0
3.5
3.0
2.5
2.0
0
10
20
30
40
50
60
70
80
No. of Oscillations

Table 9.

Partition Coefficients of MT-II at Different pH Values

Oil Phase	Partition Coefficients (P.C.)		
	pH 4.57	pH 7.35	pH 12.20
Octanol	0.126	2.880	12.416
	0.107	2.859	12.487
	0.110	2.731	12.565
Means	0.114	2.823	12.489
SD	0.010	0.081	0.075
%CV	8.719	2.857	0.597
Isooctane	0.067	0.251	0.450
	0.074	0.232	0.406
	0.073	0.269	0.398
Means	0.071	0.251	0.418
SD	0.004	0.019	0.028
%CV	5.590	7.484	6.740
Δ Log P.C.	0.207	1.052	1.475

Figure 17.

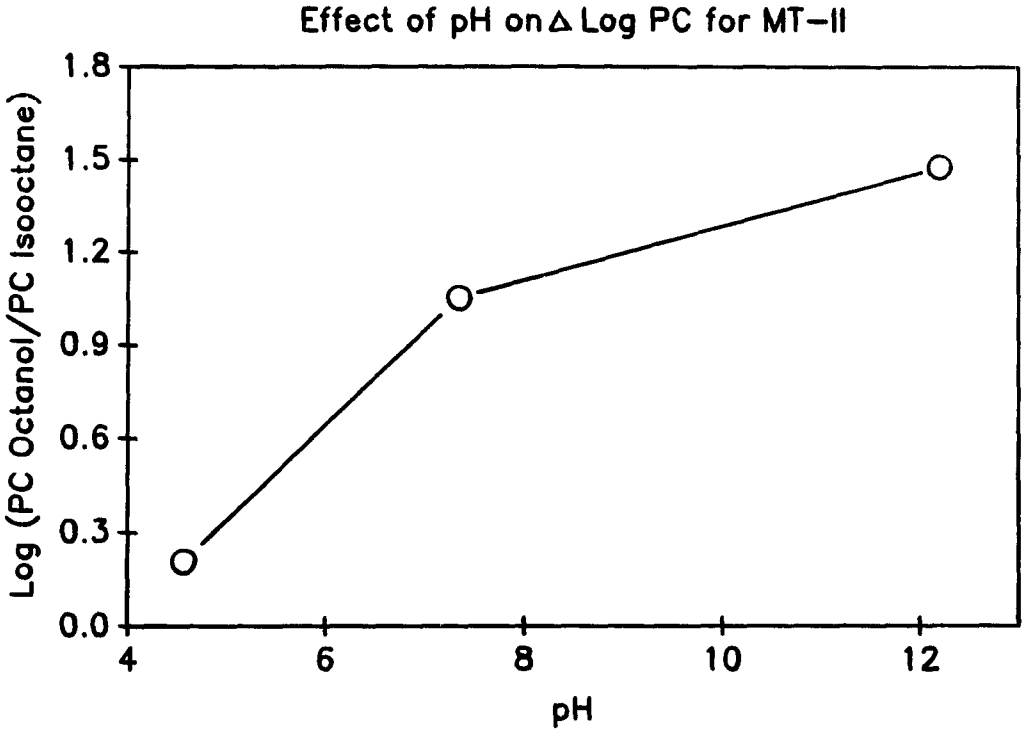
Effect of pH on Δ Log PC for MT-II
Log (PC Octanol/PC Isooctane)
1.8
1.5
1.2
0.9
0.6
0.3
0.0
4
6
8
10
12
pH

CHAPTER V

CONCLUSIONS

Peptide/protein drugs are increasingly becoming a very important class of therapeutic agents as a result of our gaining more understanding of their role in physiology and pathology as well as the rapid advances in the field of biotechnology/genetic engineering. The rational development of dosage forms for peptides depends upon a fundamental appreciation of the physicochemical properties of the peptide and its delivery system. Properly designed preformulation studies can provide important information relevant to the selection of the most appropriate formulation strategies. This investigation has evaluated some important physicochemical properties of Melanotan-II. Since temperature, pH value, and phosphate buffer concentration can affect the stability of MT-II, those parameters should be carefully considered in the final formulation. The pK_{a1} and pK_{a2} values help us to predict the behavior of MT-II at different pH values and to estimate the permeability across biological menbranes. One major purpose of preformulation studies is to identify which of the possible routes of administration may be the most feasible. The traditionally preferred mode of delivery of a pharmaceutical drug has been by the oral route. However, most peptide/protein drugs are easily degraded by proteolytic enzymes in the gastrointestinal tract and thus are generally not suitable for oral administration. However, the simulated gastric juice test of MT-II showed a good stability to hydrochloric acid and pepsin. The partition coefficient data suggested a high permeability of MT-II across gastrointestinal membranes at physiologic pH. Based upon the results of these preformulation studies, the oral route of administration seems an attractive possibility and is therefore worthy of further study.

APPENDIX

Abbreviations of Amino Acids

Arg:	arginine
Glu:	glutamic acid
Gly:	glycine
His:	histidine
Lys:	lysine
Met:	methionone
Nle:	norleucine
Phe:	phenylalamine
Pro:	proline
Ser:	serine
Trp:	tryptophan
Tyr:	tyrosine
Val:	valine

LIST OF REFERENCES

Albert, A. and Serjeant, E.P.(1971) The determination of ionization constants. Chapman and Hall Ltd. Press, London, 1-64.

Al-Obeidi, F, Castrucci, A.M.L., Hadley, M.E., and Hruby, V.J. (1989) Potent and prolonged acting cyclic lactam analogues of α-melanotropin: design based on molecular dynamics. J. Med. Chem., 32, 2555-2561.

American Cancer Society (1991) Cancer facts and figures-1991., 12.

Anik, S.T. and Hwang, J. (1983) Adsorption of D-Nal(2)^6 LHRH, a decapeptide, onto glass and other surfaces. Int. J. Pharm., 16, 181-190.

Bailey, P.D. (1990) An introduction to peptide chemistry. Wiley Publishers Science Press, New York, 1-10, and 182-191.

Bodanszky, M. (1988) Peptide chemistry. Springer-Verlag Press, New York, 1-9, 39-52.

Bundgaard, H. and Møss, J. (1990) Prodrugs of peptides 6.: Bioreversible derivatives of thyrotropin-releasing hormon (TRH) with increased lipophilicity and resistance to cleavage by the TRH-specific serum enzyme. Pharm. Res., 7, 885-892.

Banga, A.K. and Chien, Y.W. (1988) Systemic delivery of therapeutic peptides and proteins. Int. J. Pharm., 48, 15-50.

Burton, P.S., Conradi, R.A., and Hilgers, A.R. (1991) Transcellular Mechanism of peptide and protein absorption: passive aspects. Drug Delivery Revs., 7, 365-386.

Burton, P.S., Conradi, R.A., Hilgers, A.R., Ho, N.F.H., and Maggiora, L.L. (1992) The relationship between peptide structure and transport across epithelial cell monolayers. J. Control. Rel., 19, 87-98.

Carstensen, J.T. (1990) "Preformulation" in Modern Pharmaceutics, Ed., Banker G.S., and Rhodes, C.T., Marcel Dekker, Inc. Press, New York, 239-262.

Chan, S.Y. and Li, W.P.A. (1989) Prodrugs for dermal delivery. Int. J. Pharm., 55, 1-16.

Chauen, V.S., Sharma, A.K., Ana, K., Paul, P.K.C., and Balaram, P. (1987) Conformations of dehydrophenylalanine containing peptides. Int. J. Peptide Protein Res., 29, 126-133.

Chien, Y.W. (1992) Novel drug delivery systems. Marcel Dekker, Inc. Press, New York, 631-745.

Chien, Y.W., Siddiqui, O., Shi, W.M., Lelawongs, P., and Liu, J.C. (1989) Direct current iontophoretic transdermal delivery of peptide and protein drugs. J. Pharm. Sci., 78, 376-383.

Cody, W.L., Wilkes B.C., and Hruby, V.J. (1984) Reversed-phase high-performance liquid chromatographic studies of a-MSH fragments. J. Chromatogr., 314, 212-231.

Connors, K.A. (1981) The study of reaction kinetics. J. Parenteral Sci. Technol., 35, 186-208.

Conradi, R.A., Hilgers, A.R., Ho, N.F.H., and Burton, P.S. (1991) The influence of peptide structure on transport across Caco-2 cells. Pharm. Res., 8, 1453-1460.

Dawson, B.V., Hadley, M.E., Kreutzfeld, K., Dorr, R.T., Hruby, V.J., Al-Obeidi, F., and Don, S. (1988) In vitro transdermal delivery of a melanotropic peptide through rat skin. Life Sci., 43, 1111-1117.

Dawson, B.V., Hadley, M.E., Levine, N., Kreutzfeld, K.L., Don, S., Eytan, T., and Hruby, V.J. (1990) In vitro transdermal delivery of a melanotropic peptide through human skin. J. Invest. Dermatol., 94, 433-435.

Damge, C., Michel, C., Aprahamian, M., and Couvreur, P. (1988) New approach for oral administration of insulin with polyalkylcyanoacrylate nanocapsules as drug carrier. Diabetes, 37, 246-251.

Dorr, R.T., Dawson, B.V., Hadley, M.E., Levine, N., and Hruby, V.J. (1988) Toxicologic studies of a superpotent α-melanotropin, [Nle^4, D-Phe^7] α-MSH. Invest. New Drugs, 6, 251-258.

Dorr, R. T. and Dawson, B.V. (1989) Results of a 30 day toxicology and pharmacokinetic study of Melanotan-II^R (Acetyl-Nle-Asp-His-D-Phe-Arg-Try-Lys-NH2) Given subcutaneously and orally in adult rodents. Toxicology report. Arizona Cancer Center, University of Arizona.

Eppstein, D.A. and Longenecker, J.P. (1988) Alternative delivery systems for peptides and proteins as drugs. CRC Critical Reviews in Therapeutic Drug Carrier Systems, 5, 99-139.

Freeke Hamelijnck, M.A., Stevenson, P.J., Kadaba, P.K., and Damani, L.A. (1992) Triazolines. XXI: preformulation degradation kinetics and chemical stability of a novel triazoline anticonvulsant. J. Pharm. Sci., 81, 392-396.

Griego, R.D. and Levine, N. (1992) Subcutaneous administration of a potent synthetic melanotropin influences human skin darkening without sunlight exposure. J. Invest. Dermatol., 98, 645, Abstract No. 560.

Hadley, M.E., Marwan, M.M., Al-Obeidi, F., Hruby, V.J., and Castrucci, A.M.L. (1989) Linear and cyclic a-melanotropin [4, 10] fragment analogue that exhibits superpotent and residual activity. Pigment Cell Res., 2, 478-484.

Hadley M. E., Wood, S.H., Lemus-Wilson, A.M., Dawson, B.V., Levine, N., Dorr, R.T., and Hruby, V.J. (1987) Topical application of a melanotrpic peptide induces systemic follicular melanogenesis. Life Sci., 40, 1998-1895.

Hansch, C. and Dunn, W.J. (1972) Linear relationships between lipophilic character and biological activity of drugs. J Pharm. Sci., 61, 1-19.

Helm, V.J. and Müller, B.W. (1990) Stability of gonadorelin and triptorelin in aqueous solution. Pharm. Res., 7, 1253-1256.

Hruby, V.J., Sawyer, T.K., Yang, Y.C.S., and Bregman, M.D. (1980) Synthesis and structure-function studies of melanocyte stimulating hormone analogues modified in the 2 and 4(7) positions: comparison of activities on frog skin melanophores and melanoma adenylate cyclase. J. Med. Chem., 23, 1432-1437.

Hruby, V.J., Kazmierski, W., Kawasaki, A.M., and Matsunaga, T.O. (1991) "Synthetic chemistry and the design of peptide-based drugs", in Peptide Pharmaceuticals, Ed., Ward, D., Elsevier Science Publishing Co., Inc., New York, 135-184.

Hussain, M.A., Shenvi, A.B., Rowe, S.M., and Shefter, E. (1989) The use of alph-aminoboronic acid derivatives to stabilize peptide drugs during their intranasal absorption. Pharm. Res., 6, 186-189.

Junginger, H.E. (1990). Bioadhesive polymer systems for peptide delivery. Acta Pharm. Technol., 36 (3), 110-126.

Lachman, L., Deluca, P., and Akers, M.J. (1986) "Kinetic principles and stability testing." in The Theory and Practice of Industrial Pharmacy, Eds., Lachman, L., Lieberman, H.A., and Kanig, J.L., Lea & Febiger Press. Philadelphia, PA. 760-803.

Lebl, M., Cody, W.L., and Hruby, V.J. (1984) Cyclic melanotropins part vi: reverse-phase HPLC studies. J. Liq. Chromatogr., 7, 1195-1210.

Lee, V.H.L. (1991) Trends in peptide and protein drug delivery. Biopharm., 4 (3), 22-25.

Levine, N., Sheftel, S.N., Eyten, T., Dorr, R.T., Hadley, M.E., Weinrach, J.C., Ertl, G.A., Toth, K., McGee, D.L., and Hruby, V.J. (1991) Induction of skin tanning by subcutaneous administration of a potent sythetic melanotropin. J.A.M.A., 266, 2730-2736.

Marwan, M.M., Abdel-Malek, Z.A., Kreutzfeld, K.L., Hadley, M.E., Wilkes, B.C., Hruby, V.J., and Castrucci, A.M.L. (1985) Stimulation of S-91 melanoma tyrosinase activity by superpotent α-melanotropins. Mol. Cell. Endocrinol., 41, 171-177.

Metzler, C. and Weiner, D. (1986) Software for the statistical analysis of nonlinear models. Am. Stat., 40, 52.

Mizutani, T. (1981) Estimation of protein and drug adsorption onto silicone-coated glass surfaces. J. Pharm. Sci., 70, 493-496.

Mizutani, T. and Mizutani A. (1978) Estimation of adsorption of drugs and proteins on glass surfaces with controlled pore glass as a reference. J. Pharm. Sci., 67, 1102-1105.

Nacht, S. (1991) Melanin, nature's own sunscreen polymer. in Cosmetic and Pharmaceutical Application of Polymers, Ed., Gebelein, C.G., Cheng, T.C., and Yang, V.C., Plenum Publishing Corporation, New York, 83-94.

Pearlman, R. and Nguyen, T. (1992) Pharmaceutics of Protein drugs. J. Pharm. Pharmacol., 44, 178-185.

Powell, M.F., Sanders, L.M., Rogerson, A., and Si, V. (1991) Parenteral peptide formulations: chemical and physical properties of native luteinzing hormone-releasing hormone (LHRH) and hydrophobic analogues in aqueous solution. Pharm. Res., 8, 1258-1263.

Ravin, L.J. and Radebough, G.W. (1990) "Preformulation", in Remington's Pharmaceutical Sciences, Ed., Gennaro, A.R., Mack Publishing Company, Easton, PA. 1435-1450.

Ruwart, M.J., Rush, B.D., Wilkson, K.F., Lakings, D.B., Zhong, W.Z., and Closson, S.K. (1989) Absolute bioavailability of the renin inhibitory peptide U-71038 in conscious rats with chronic bile duct canula, Pharm. Res., 6, S-227.

Rytting, J.H. (1989) Penetration/absorption enhancers for nasal and rectal delivery of peptides and proteins. J. Pharm. Sci., 78, 888.

Saffran, M., Kumar, G.S., Savariar, C., Burnham, J., Williams, F., and Neckers, D.C. (1986) A new approach to the oral administration of insulin and other peptide drugs. Science, 233, 1081-1084.

Sawyer, T.K., Sanfilippo, P.J., Hruby, V.J., Engel, M.H., Heward, C.B., Burnett, J.B., and Hadley, M.E. (1980) 4-Norleucine, 7-D-phenylalanine-α-melanocyte-stimulating hormone: a highly potent α-melanotropin with ultralong biological activity. Proc. Natl. Acad. Sci. USA, 77, 5754-5758.

Seymour, M.D., Clayton, J.W., and Fernando, Q. (1977) Determination of pKa values of acid components in atmospheric condensates by linearization of segmented titration curves. Anal. Chem., 49, 1429-1432.

Spencer, R.P. (1960) Enzymes and digestive process. in The intestinal tract. published by Thomas, C.C., Springfield, IL, 107-126.

Theodorakis, M.C., Digenis, G.A., Beihn, R.M., Shanbhu, M.B., and Deland, F.H. (1980) Rate and pattern of gastric emptying in humans using ^{99m}Tc-labelled triethylenetetraamine-polystyrene resin. J. Pharm. Sci., 69, 568-571.

Ugwu, S.O. and Blanchard, J. (1992) An HPLC assay for the α-melanotropin [4, 10] fragment analogue (Melanotan-II) in rat plasma. J. Chromatogr., in press.

U.S. Pharmacopeia National Formulary (1980) USPXX/NFXV, 1105.

Wadke, D.A., Serajuddin, A.T.M., and Jacobson H. (1989) "Preformulation testing", in Pharmaceutical Dosage Forms: Tablets, Eds., Lieberman, H.A., Lachman, L. and Schwartz, J.B., Marcel Dekker Inc., New York, 1-73.

Wang Y.J. and Hanson M.A. (1988) Parenteral formulations of proteins and peptides: stability and stabilizers. J Parenteral Sci. Technol. 42, Supplement 4-26.

Won, C.M. (1992) Kinetics of degradation of levothyroxine in aqueous solution and in solid atate. Pharm. Res., 9, 131-137.